MAPPING THE SUSCEPTIBILITY TO SLOW-MOVING LANDSLIDES ON Oʻ AHU

A SUBMITTAL TO THE GRADUATE DIVISION OF THE UNIVERSITY OF HAWAIʻI AT MĀNOA IN PARTIAL FULFILLMENT OF THE REQUIREMENTS FOR THE DEGREE OF

MASTER OF GEOSCIENCE FOR PROFESSIONALS

MAY 2018

By

Elise Leroux

Committee:

Garrett Apuzen-Ito (Chair)

Scott Rowland

Masanobu Fujioka

Mapping the Susceptibility to Slow-Moving Landslides on O‘ahu

Master of Geoscience for Professionals

Elise Leroux

Abstract

Slow-moving landslides in residential areas on O‘ahu have resulted in the losses of dozens of homes and millions of dollars. In most cases, the landslide was not noticed prior to development due to the extremely slow and episodic motion, and lack of reference points; or because the movement initiated during or after development. As the population on the island grows, construction continues to expand into areas that are marginally suited for development. There is currently no map to indicate areas prone to slow-moving landslides. To address this shortcoming, we examined seven previously identified slow-moving landslides in southeast O‘ahu for relationships among seven parameters for which data are available in GIS-readable format: soil type, type of geologic formation, slope, average infiltration rate, aspect (azimuth of the normal to the surface), average solar radiation, and elevation. We conducted numerical or statistical analyses to “score” the parameters, with a higher score representing more commonality among the seven landslides. We then summed the scores of the above parameters at each landslide to produce a total “susceptibility score” of the common characteristics shared among known slow-moving slides. The resulting “Slow-Moving Landslide Susceptibility” maps, created in ArcGIS, depict which areas are more or less susceptible to slow-moving landslides based on the characteristics of the seven mapped slides. The maps lack the precision to be useful on a localized scale, but they identify general areas of susceptibility, some of which are currently undeveloped. The maps are intended as a tool for developers, engineers, and regulators to use to 1) inform development criteria, and 2) guide engineering design to mitigate soils and structures against potential slide movement.

Table of Contents

List of Figures

List of Tables

1.0 INTRODUCTION AND MOTIVATION

Slow-moving landslides have been causing problems in residential areas of O‘ahu since at least the 1950s [*Peck*, 1959]. These landslides are usually not detected in undeveloped areas; they are often only detected after construction. Furthermore, grading and other site improvements accompanying development may contribute to the initiation of movement. Whereas some of the known landslides have been studied extensively, and the United States Geological Survey (USGS) explored common characteristics of slow-moving landslides in the Honolulu district in the early 1990s [*Ellen et al*., 1995], little has been done to define areas that may be susceptible to such sliding in the future so that engineers, developers, and planners may design accordingly.

There are many types of mass wasting, of which landsliding is one. The more spectacular landslides are those that happen rapidly, sometimes resulting in major and sudden destruction. Slow-moving landslides, on the other hand, form and progress slowly. Previous studies in Honolulu describe several characteristics which, taken together, describe this type of slide. These characteristics are summarized in *Ellen et al*. [1995]: 1) These slides form over years to decades; 2) Movement rates – when active – are typically about 0.25 inch per day, but may be as great as 1 inch per day; 3) Movement is episodic and correlated to rainfall, with total downslope movement in an episode typically several feet or less (not tens of feet); 4) These slides do not accelerate into rapid debris flows; 5) These slides occur in relatively gently sloping surficial colluvial deposits along valley margins, near the base of steep valley walls; 6) The slides often enlarge progressively from one or more small localized areas; 7) The depth of the slide surface typically ranges 20-30 feet, but may be as shallow as 15 to as deep as 60 feet; 8) The basal slip surfaces generally form in highly plastic clay or silty clay, but may pass through clayey silt; and 9) The head scarps and toes are distinct, but flanks may be obscure.

Early investigations of slow-moving landslides on O‘ahu focused on two landslides that occurred in new developments in Honolulu in the 1950s and 1960s: the Waiomao Slide in Pālolo Valley (subdivision completed late 1952; problems noticed by March 1954) [*Peck*, 1959] and the Hind Iuka landslide in ‘Āina Haina (development approved 1956; movement noticed in early 1966) [*Peck*, 1968]. Whereas those two landslides were studied and remedial measures attempted, few studies were conducted on a regional scale. The 1987 New Year’s Eve storm, which had excessively high rainfall, caused many debris flows and triggered noticeable episodes of movement in slow-moving landslides. This led to renewed efforts – and funding – to characterize slow-moving landslides in the Honolulu district. The efforts were primarily led by USGS in cooperation with City & County of Honolulu, and included several studies conducted in the late

1980s and early 1990s related to individual landslides (e.g., *Baum and Reid*, 1992; *Baum and Reid*, 1995).

Baum and Reid [1995] of the USGS describe a detailed three-year study of the Alani-Paty landslide in Mānoa, which appeared to have many of the characteristics typical of the known slow-moving landslides on O‘ahu. The Alani-Paty slide formed within the gently sloping debris apron between the flat valley floor and the steep slope of exposed basalt. The debris apron is formed by intermittent rock falls and debris flows, which include weathered clasts and soil. The materials consist of crudely stratified clayey silt and silty clay containing weathered basalt boulders, cobbles, and gravel. Once deposited, the materials weather and form vertisols, which contain at least 30% clay by weight and are highly expansive. The debris aprons contain weak layers parallel to the slope, and the clays at the basal slip surface were found to have low shear strength. Most of the landslide material was found to be perennially saturated, although materials underlying the landslide were largely unsaturated or had low pressure heads. However, perched water was not found uniformly in the material, and pressure heads in piezometers with tips within the landslide did not respond uniformly to rainfall. Despite the landslide material being saturated year-round, landslide movement during the study occurred only during rainy periods. Not all rainy periods resulted in detectable movement; the episodes of movement occurred after periods of intense rainfall during storms that lasted several days.

The USGS conducted a study to characterize known slow-moving landslides and areas susceptible to sliding. The study, *Relation of slow-moving landslides to earth materials and other factors in valleys of the Honolulu District of Oahu, Hawaii* [USGS Open-File Report 95-218] by Stephen D. Ellen, Lori S.M. Liu, Robert W. Fleming, Mark E. Reid, and Mark J. Johnsson, prepared in cooperation with the City and County of Honolulu, Department of Public Works, published in 1995, was the starting point for our study. *Ellen et al* [1995] looked at mapping of surface soils, geologic mapping, rainfall, slope, and subsurface data (boring logs and test pit logs).

Ellen et al. [1995] identified twelve known or probable (referenced in previous literature but not identified in the field by USGS) slow-moving landslides in the Honolulu District, seven of which were active at the time of, or shortly prior to, the study, and five of which had been previously identified in PhD dissertations by De Silva [1974] and Jellinger [1977]. *Ellen et al*. [1995] determined that the slow-moving landslides tended to occur where the following conditions were met: 1) intermediate slope “aprons” between steep valley walls and gradual valley floors; 2) rainfall between 1 and 2 meters per year; 3) geologic material is mapped as alluvium; and 4) soils developed in this alluvium are vertisols (Figure 1). Based on those conclusions, *Ellen et al* [1995] hypothesized that failure surfaces have formed in buried vertisols because vertisols in the subsurface provide slope-parallel horizons of weak, highly plastic expansive clay; and low permeability in the material creates favorable surfaces for perching water, resulting in likely slip surfaces.

Vertisols form only under specific climatic conditions, particularly in areas of low to moderate rainfall that occurs seasonally (i.e. where there are alternate periods of wetting and drying); therefore, these soils do not develop in areas that are perennially wet or perennially dry. *Ellen et al.* [1995] suggested that correlation between surface and subsurface vertisols should coincide in general, if paleoclimate was similar to today’s climate, which they hypothesized it was – meaning that surface vertisols are likely a good indicator of subsurface vertisols.

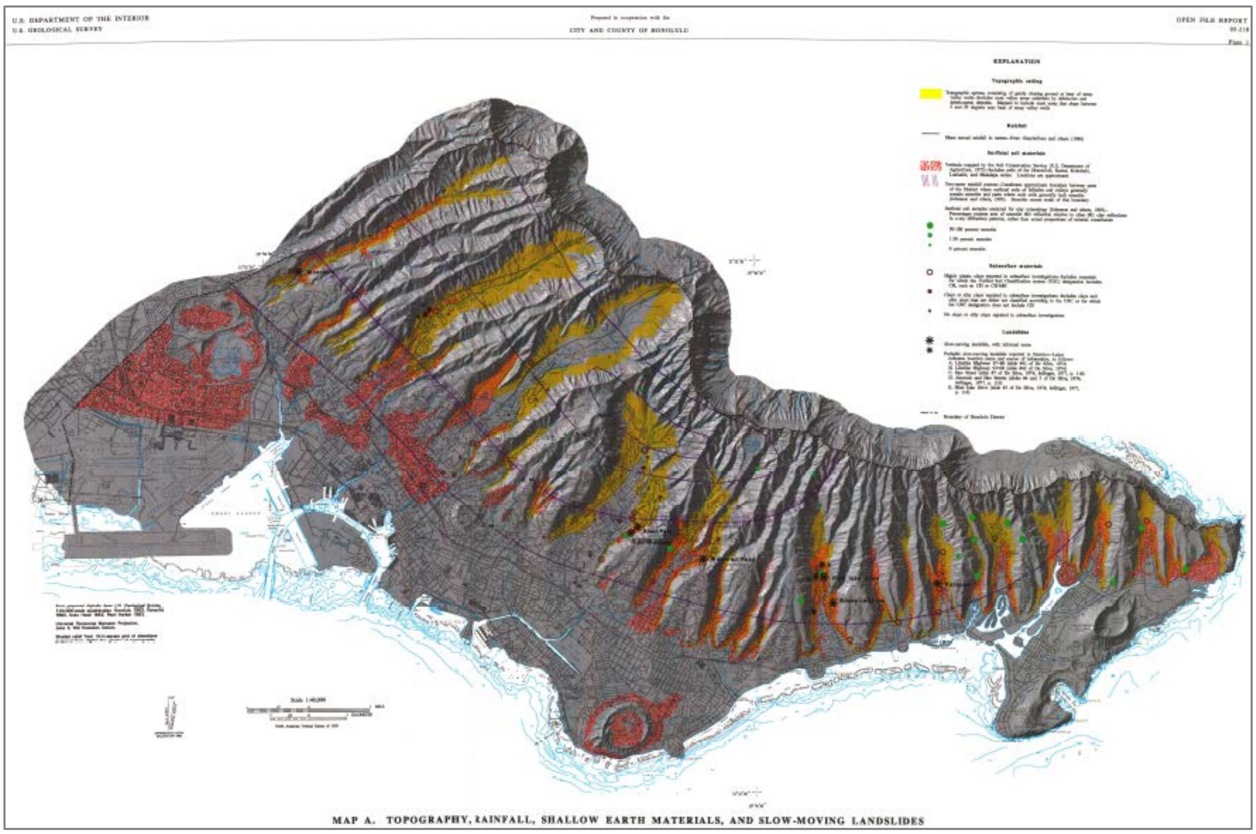

Figure 1. Map A from *Ellen et al.* [1995].
Yellow indicates “topographic aprons” including most areas of slopes between 5 and 25 degrees near the base of steep valley walls; red represents approximate locations of mapped vertisols; purple lines are isohyets, with the 2 m isohyet indicated by diagonal hachures.

As part of their study, *Ellen et al.* [1995] reviewed more than 1,000 boring and test pit logs from more than 50 sites in valleys throughout their study area of Southeast O‘ahu. The subsurface data – which were not published as part of the report because they were proprietary – were of variable quality and had wide spatial variation; therefore, the authors had to generalize the information. They compared the subsurface data from throughout the valleys to borings in the Alani-Paty landslide, which they determined to be representative of the slow-moving landslides in their study. They found that materials in the landslides are similar to materials throughout the valleys, and that typical subsurface data (boring / test pit logs and laboratory tests) collected for engineering purposes do not isolate any materials that are unique to landslides. Therefore, they concluded that areas of likely movement cannot be predicted from compiled subsurface data, and delineation of such areas would require new investigations that look specifically for materials or conditions critical to landsliding.

Subsequent to the publication of *Ellen et al.* [1995], the USGS proposed to create an Engineering Geologic Map and Map of Relative Slope Stability or landslide susceptibility map for the Honolulu District [*Rex Baum*, USGS, personal communication, April 2017]. That study was never funded and the work was not conducted. To our knowledge, the only studies subsequent to 1995 have been related to individual slides, soil properties, or correlating rainfall to landslides (but not solely to slow-moving landslides) [*Deb and El-Kadi*, 2009]; and no additional work has been conducted to analyze multiple slow-moving landslides or to identify areas where these types of slides may occur in future. There is currently no one in USGS’ Honolulu office working on landslides [*Chui Ling Cheng*, USGS, personal communication, April 2017].

If a map can be produced that indicates areas having the potential for slow-moving landslides, then development strategies, and/or engineering design could be used to mitigate structures against slide movement. Without this knowledge, for example, construction of a typical residential structure at the foot of a steep slope may not require a geotechnical investigation; and if one is conducted, a geotechnical engineer may sample only near-surface soils due to the light nature of the proposed residential structure. However, if the area were known to potentially be susceptible to slow-moving landslides, it is likely that a more detailed or deeper investigation would be performed, and engineering design would be conducted so that the surface soils could be replaced or reinforced, and/or so structures are supported on deep foundations that bear on rock underlying the susceptible soils.

The objective of this Master of Geoscience for Professionals (MGeo) project is to develop a Slow-Moving Landslide Susceptibility Map to identify areas that share characteristics with known slow-moving landslides and thus are likely susceptible to slow-moving landslides in the future. We developed this map, as well as multiple supporting maps, through compilation and analysis of geographic information system (GIS) data to determine common characteristics of slow-moving slides such as slope, soil type, and surficial geology, among others. We then used the analysis to assess which areas have similar characteristics but may have not been known to slide, in some cases possibly because they have not yet been developed.

2.0 PARAMETERS AND PROCESSING METHODS

2.1 Parameter Selection

Table 1 lists data types, or parameters, that we used in the quantitative analyses conducted to produce the Slow-Moving Landslide Susceptibility Map. A detailed discussion of each parameter follows in Section 3.2. Several parameters (Table 2) were considered but not used in the final analyses. Some of them were analyzed qualitatively**.**

Table 1. Parameters used in quantitative analyses, and rationale for use.

Parameter	**Rationale for use**
Geologic material	Identified by *Ellen et al* [1995] as an important factor in slow-moving landslides: they determined that all the slides were in or near areas mapped as alluvium.
Soil Order	Identified by *Ellen et al* [1995] as an important factor in slow-moving landslides: they determined that all the slides were at or immediately adjacent to areas mapped as vertisols, which are characterized by high shrink-swell potential and low shear strength.
Slope	Identified by *Ellen et al* [1995] as an important factor in slow-moving landslides: in particular, slopes that were neither the steepest nor most gradual in a valley are more susceptible to sliding.
Infiltration	Rainfall was identified by *Ellen et al* [1995] as an important factor in slow-moving landslides. However, the USGS recently developed a model that allows for calculation of infiltration, which includes rainfall. We determined for this study that the amount of water entering the surface of the landslides (i.e., infiltration) would be more important than rainfall.
Aspect (azimuth of the normal to the surface)	The majority of slow-moving landslides in our study (five out of seven) are on the east sides of valleys, and there has been some speculation that the aspect could be a factor in the wetting and drying of the soils, promoting the development of vertisols and the shrink-swell soil behavior that contributes to slope movement.

Parameter	Rationale for use
Solar Radiation	As with aspect, solar radiation may be a factor in the wetting and drying of soils. A qualitative review of data indicated that the slides all fell within a similar range of solar radiation, and therefore it may be a factor in development of the landsliding.
Elevation	A qualitative review of data suggested that the elevation range of the slides may be a limiting factor because they are all within a relatively small range.

Table 2. Parameters not used in quantitative analyses, and rationale for omission.

Parameter	Rationale for omission
Rainfall	Although rainfall is one of the parameters identified by *Ellen et al* [1995], it was omitted from our analysis because it is incorporated in infiltration.
Land cover	Land cover, which includes vegetation, was reviewed qualitatively, but all the known slow-moving landslides are in developed areas. Therefore, this parameter could not be used as a predictive parameter for landslides in areas currently undeveloped.
Recharge	Recharge is the amount of water expected to pass through the soil and recharge the groundwater aquifer. Mapping recharge values from *Engott* [2017] (GIS shapefile of mean annual water-budget components of O‘ahu, USGS) initially showed promise due to recharge anomalies appearing in some of the landslide areas, but the reasons for the anomalies could not be fully determined. Additionally, discussions with USGS personnel who had developed the shapefile and produced the associated report [*Engott et al.*, 2017], resulted in the use of infiltration as a better estimation for the water retained in the soils.
Composition of clay-size fraction of material	Subsequent to *Ellen et al* [1995], *Wan et al.* [2002] found that the fraction of clay-sized material in one or more of the slow-moving landslides in Hawai‘i is actually predominantly amorphous silica-rich material that is not yet clay mineralogically, and this largely influences the plasticity and shrink-swell behavior of the colluvial soils. *Wan and Kwong* [2002] hypothesized that the slope failure in a slow-moving landslide is “likely to involve primarily the rupture of the strong interparticle bonds provided by the amorphous clay-size materials during the softening process. Thus, the shear zone formed in the field should be a zone of high water content with very little cohesive strength.” Further, the properties of the soils with these amorphous materials, including shear strength, have large variations. The presence of these amorphous materials may be an indicator of potential for slow-moving landslides [*Kaya*

Parameter	Rationale for omission
	and Kwong, 2007]. However, the presence of amorphous material in the clay-sized fraction of colluvial soils, although it may be an important factor in these slow-moving landslides, was not used in our study because of impracticality of collecting these data both for multiple existing slides and for others areas that may be susceptible to sliding. It would be necessary to obtain soil samples, then analyze them using x–ray diffraction. This is not a method used for typical evaluation of soil properties in geotechnical engineering: most local engineering firms who may be evaluating areas for construction would not have access to equipment or expertise to conduct similar tests.

2.2 Parameter Data Sources and Data Processing

We conducted much of the data assessment and processing using Esri® GIS mapping software: ArcMap version 10.5.1 (student version, which includes all extensions). Maps are in the NAD_1983_HARN_StatePlane_Hawaii_3_FIPS_5103_Feet projection, primarily because it is the standard projection used by land surveyors on O‘ahu. First, we conducted qualitative mapping and analyses to inform appropriate approaches to data processing. Following mapping, reprojection, and clipping, we compiled and analyzed the data to assess commonalities among slides. Based on qualitative review, we selected seven parameters that could potentially predict development of slow-moving landslides. Table 3 presents parameters, the spatial resolution of each, and processing methods.

For each of the seven parameters (Table 1), we defined susceptibility scores (ranging from 0 and 100) for each parameter. Details of how the scores were established are presented in the following sections in which individual parameters are discussed. After determining susceptibility scores, we reclassified each of these datasets in ArcMap. We then weighted the reclassified layers based on their relative importance, then summed the weighted scores to produce the Slow-Moving Landslide Susceptibility Maps. We discuss the details of the reclassification, susceptibility scoring, and weights in detail later and do not include them in Table 3.

Table 3. Parameters, source, resolution, and processing methods.

Parameter	Source and resolution	Data processing
Geology	*Sherrod et al* [2007]. Geologic Map of the State of Hawaiʻi, and associated shapefiles, published by USGS.	• We re-projected the shapefile into the datum of the map and clipped it to the island of O‘ahu.

Parameter	Source and resolution	Data processing
	According to the explanatory pamphlet accompanying the map: “Accuracy ranges widely across the map. For most of the islands, contacts should be considered ‘approximately located,’ with standard error of 100 m (plus or minus 50 m)… The new mapping from West O‘ahu and East Maui ranges in accuracy from 15 to 50 m.”	• We selected alluvium (consisting of both *Alluvium*, map symbol *Qa*, and *Older alluvium*, map symbol *QTao*) and created a new feature class consisting of alluvium only. • We created a raster file from the alluvium feature class (Spatial Analyst Tools > Distance > Euclidean Distance), to a distance of 492.126 feet (150 m) from the alluvium boundaries, because the “standard error of mapping” is 100 m ± 50 m. Cell size was set at 3.28084 feet (1m).
Soil Order	*College of Tropical Agriculture and Human Resources, University of Hawai‘i* [2014]. The Soil Orders shapefile is part of the Hawai‘i Soil Atlas, which was derived from the Natural Resources and Conservation Service (NRCS) databases and websites. The map units are the same as in the NRCS soils mapping, but the division by soil orders makes it easier to separate the vertisols form other soils. Because the original mapping was at a 1:24,000 scale, we assumed that the error would be similar to that of the geologic mapping, i.e. 100m ± 50m.	• We re-projected the shapefile into the datum of the map and clipped it to the island of O‘ahu. • We selected vertisols and created a new feature class consisting of vertisols only. • We created a raster file from the vertisols feature class (Spatial Analyst Tools > Distance > Euclidean Distance), to a distance of 492.126 feet (150 m) from the vertisols boundaries. Cell size was set at 3.28084 feet (1m).
Slope	*National Geospatial-Intelligence Agency (NGA)* [2009a] and *NGA* [2009b]. Lidar-derived bare earth Digital Elevation Model (DEM) rasters at 1meter resolution.	• We converted the DEM pixel values from meters to feet, then re-projected the DEM into the datum of the map. • We used the 1-meter DEM titled “honolulu_be_southeast” for analyses of the known landslide areas; and the 1-meter DEM titled

Parameter	Source and resolution	Data processing
	DEMs at 1 m resolution are available for O‘ahu from 2009 and 2013, but neither dataset has complete coverage of the island. The 2009 version was selected for our study because all seven slides are within a single raster, which is not the case for the 2013 DEMs. *USGS* [2015]. O‘ahu DEM – 10 m raster, complete island.	“honolulu_be_southwest” in the mapping and analysis of southwest Honolulu. We used the 10-meter DEM to produce the island-wide Slow-Moving Landslide Susceptibility map. • We created a slope raster from each DEM used (3D Analyst > Raster Surface > Slope).
Infiltration	*Engott* [2017]. GIS shapefile of Mean annual water-budget components for the Island of Oahu, Hawaii, for average climate conditions, 1978-2007 rainfall and 2010 land cover. Associated with *Engott et al* [2017] report published by USGS.	• We added a field to the table associated with the shapefile to calculate infiltration, using the equation: Infiltration = Rain + Fog + Irrigation + Septic - Runoff - Canopy Evaporation. • We created a new shapefile from the infiltration data, re-projected it to the map datum, then converted it to a raster with cell size set at 3.28084 feet (1m).
Aspect	*NGA* [2009a] and *NGA* [2009b]. (Same as “Slope”.) O‘ahu lidar-derived bare earth DEM (1m resolution raster).	• We used the re-projected DEM (See “Slope”) to create Aspect from each DEM used (3D Analyst > Raster Surface > Aspect). We used the output raster for the statistical analysis. • We reclassified the aspect raster into 22.5-degree bins for display purposes and qualitative analysis.
Solar Radiation	*Giambelluca et al.* [2014], Solar Radiation of Hawai‘i: solar radiation was estimated as part of a larger project on evapotranspiration. Raster file of annual mean hourly solar radiation in W/m^2. Resolution is 250 m.	• We clipped the raster, which provides statewide data, to O‘ahu and re-projected it to the datum of the map.

Parameter	**Source and resolution**	**Data processing**
Elevation	*NGA* [2009a] and *NGA* [2009b]. (Same as “Slope”.) O‘ahu lidar-derived bare earth DEM (1m resolution raster).	• We used the re-projected DEM (See “Slope”) to create contours from each DEM used (3D Analyst > Raster Surface > Contour) at 10-foot intervals. • We created a raster of the contour shapefile to allow reclassification.

3.0 LANDSLIDE CHARACTERIZATION

We selected seven slow-moving landslides for analyses, even though there are more known slow-moving landslides in the Honolulu district [*Ellen et al.*, 1995]. We chose the seven primarily because mapped slide boundaries were available. Additionally, the locations of other known slow-moving landslides could be used to check the analytical results of our study, as an evaluation of the susceptibility maps. For proprietary reasons, one of the landslides in our study cannot be named, nor can its location be provided. We term this slide “Slide 7” throughout our report. The names and locations of the other six slow-moving landslides are shown in Figure 2.

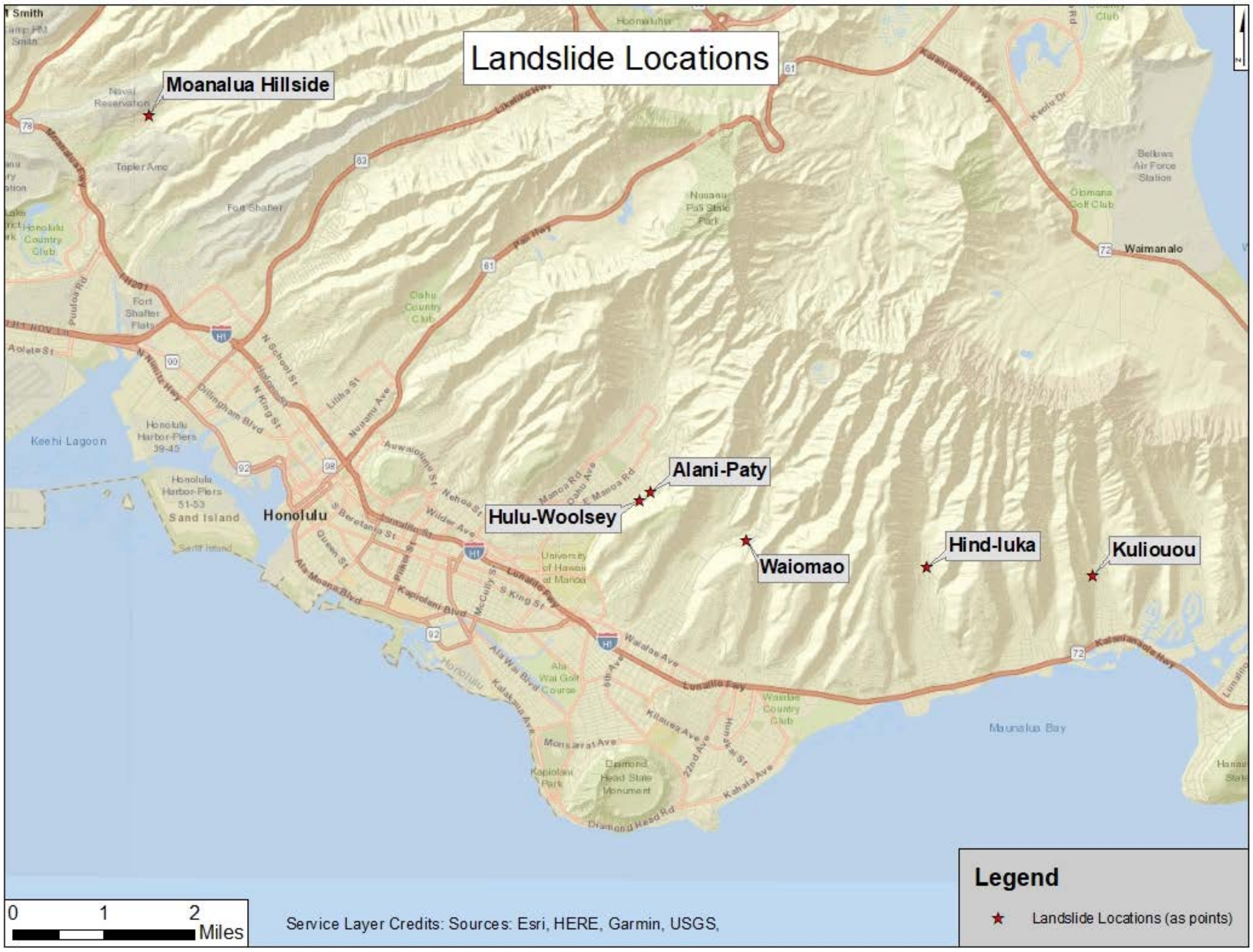

Figure 2. Locations of six of the studied slow-moving landslides. Slide 7 is not depicted.

3.1 Delineating Slide Areas and Defining Local Study Areas

Mapping of landslides boundaries was based on previous reports (Table 4), with the exception of the Slide 7, which we mapped in the field. We scanned maps from reports by others, then geo-referenced the maps to high-resolution aerial imagery from Pictometry, Inc. provided under license to the MGeo author’s employer, Masa Fujioka & Associates. We then traced approximate landslide boundaries. Disadvantages of this method are: 1) the boundary is only as accurate as the mapping, which was done by others; geo-referencing to imagery typically adds some uncertainty; and some of the maps are old and landslides boundaries may have expanded. Advantages of this method are: 1) remediation (such as repairs to structures and roads) and access issues may make it more difficult to map the landslides now than when they were studied; and 2) time limitations prohibited extensive fieldwork.

Table 4. The seven slow-moving landslides analyzed, and the source of the slide boundaries.

Slide Name	**Location (Region of Honolulu)**	**Source of Slide outline**	**Side of Valley**
Alani-Paty	Mānoa	*Baum and Reid* [1992]. Plate 2.	East
Hind Iuka	ʻĀina Haina	*Peck* [1968]. Fig. 1.	East
Hulu-Woolsey	Mānoa	*Lyon Associates, Inc.* [2014]. Figure 1.	East
Kuliouou	Kuliʻouʻou	*Brandes* [2012]. Figure 2.	West
Moanalua Hillside	Moanalua	*Lyon Associates, Inc*. [2015]. Figure 1.	West
Slide 7	--	Mapped by MGeo author in course of work for Masa Fujioka & Associates. No report produced.	East
Waiomao	Pālolo	*Geolabs, Inc.* [2015]. Figure 2.	East

We defined approximate watersheds from which surface runoff enters the landslide areas in ArcMap, using Spatial Analysis Hydrology tools as follows. We produced "flow direction" lines from the 1-meter DEM, indicting where surface runoff would flow, and created "sinks" to assess if there were low areas. We did not observe any sinks that appeared to be anything other than processing artifacts; therefore, we filled the sinks and produced a new set of flow direction lines. We used these lines to create "flow accumulation" lines, which represent places where surface runoff would accumulate, i.e. ephemeral streams. Next we created "pour points" along the flow accumulation lines, to calculate all areas from which surface runoff would reach a given pour point, i.e., to define the watershed that contributes to the point. Pour point locations were determined by trial and error, to best identify watersheds that contribute surface runoff to the landslide area, but without incorporating too much additional area (area that does not contribute runoff to the landslides). We then converted the output "watershed" raster to a polygon feature class. In cases where there were multiple watersheds feeding into a single slide outline, we merged them into a single polygon. Because this process creates watersheds based on points, it does not create a perfect overlap with the landslide areas, which are polygons. Landslide boundaries and watersheds are depicted in Figure 3.

For two of the slides, Slide 7 and Moanalua Hillside, the resulting watersheds are not much larger than the slide areas. This is because both have roads upslope of them which, based on the ArcMap Hydrology tool results, are expected to intercept stormwater runoff from the hillslopes above the roads. However, subsurface runoff does not necessarily mimic surface runoff; therefore, the mapped watersheds for these two slides may be poor indicators of the areas that actually contribute water to the slide areas.

We clipped datasets by both landslide boundaries and by watershed boundaries, and conducted qualitative analyses. In addition, we drew rough valley boundaries using a hillshade created from the DEM, and analyzed slope distributions within the valleys to compare them to slope distributions within the landslide and watershed boundaries (described in Section 3.2.2). Clipping was generally accomplished by converting the boundary polygon (slide, watershed, or valley, as applicable) to graphics, then using the window/image analysis tool to clip the raster or shapefile for additional analysis.

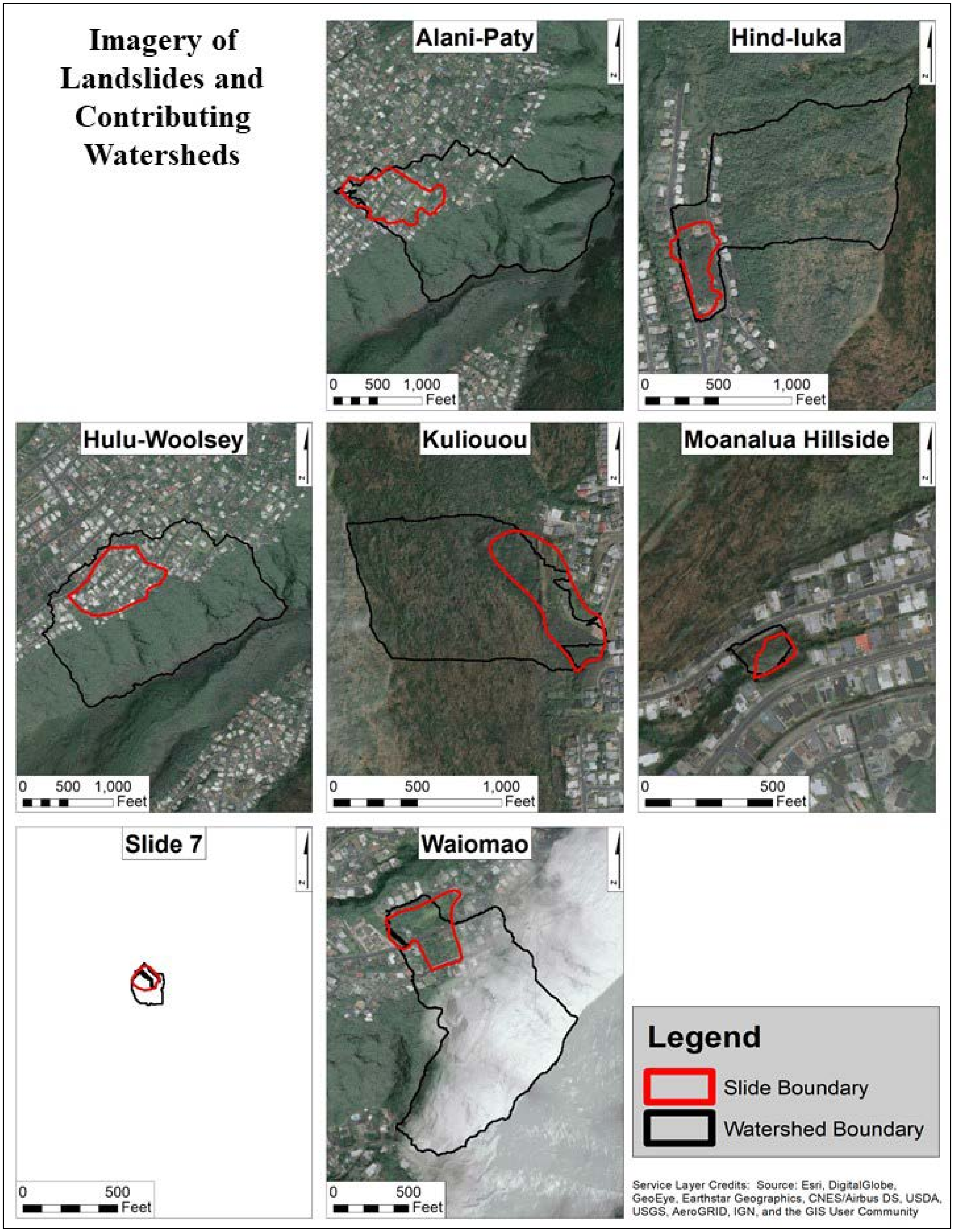

Figure 3. Boundaries of the seven slow-moving landslides analyzed in this study, as well as their approximate contributing watersheds.

3.2 Findings

3.2.1 Geology and Soils

We conducted qualitative analysis of geologic mapping, which, along with the information from *Ellen et al* [1995], indicated that the slow-moving landslides are within or near areas mapped as alluvium. Although the material is actually colluvium, the geologic mapping does not distinguish between colluvium and alluvium – both materials are mapped as alluvium. Of the seven slides we evaluated, six are predominantly in areas mapped as alluvium (four *Older alluvium*, map symbol *QTao*; and two *Alluvium*, map symbol *Qa*) [*Sherrod et al., 2007*]. The one slide that is not predominantly within alluvium is Slide 7, which is mapped as predominantly Ko‘olau Basalt, with alluvium in the downslope corner. This slide, however, lies completely within 186 feet of mapped alluvium; which is well within the stated mapping error of 100 m (±50 m) [328.1 feet (±164 ft)].

Susceptibility scores for all parameters were defined to fall within the range 0 to 100, rounded to the nearest whole number because reclassifying in ArcMap requires use of integers. Thus, areas within the alluvium boundary are assigned a susceptibility score of 100, and areas from 0 to 186 feet of the alluvium boundary are scored 17. The ratio of 100-to-17 equals the ratio of six-to-one slides within versus just outside the alluvium boundary. All other areas where assigned a susceptibility score of 0. Details of the scoring are provided in Table 5.

Table 5. Susceptibility scoring for mapped alluvium.

Criteria	**Number of slides**	**Percent of slides**	**Susceptibility Score**
Predominantly or completely mapped as alluvium	6	85.7	100
Not predominantly alluvium but within 0-186 feet of alluvium	1	14.2	17
>186 feet from mapped alluvium boundary	0	0	0
NoData	--	--	0

There are 12 soil orders in soil taxonomy [*College of Tropical Agriculture and Human Resources, 2014*], one of which is vertisols, characterized as being expansive and having high shrink-swell potential, and another of which is ultisols, not characterized as being expansive or having high shrink-swell potential. Six of the seven slides that we evaluated are predominantly in mapped vertisols (three in the *Kaena Series*, two in the *Lualualei Series*, and one in both *Kaena* and *Lualualei Series* soils) [*USDA*, *1972*]. One of these six slides, Alani-Paty is also partly within the *Lolekaa Series* soils, which is an ultisol. Slide 7 is mapped as entirely *Lolekaa Series* soil, however, the slide boundary is approximately 120 ft from mapped vertisols at its closest point, and all of Slide 7 is within 241 feet of mapped vertisols. We assume the soils mapping has a similar margin of error to the geologic mapping, i.e. 100 m (±50 m) [328.1 ft (±164 ft)], because both were conducted at the same scale of 1:24,000.

For assigning susceptibility scores associated with soil type, we note that six of the seven slides (85.7% of the seven) are predominantly within the mapped vertisols; and 14.2% of the slides are in the 0-241 feet distance from the vertisols boundary. Thus areas within the vertisols boundary are scored 100, areas within 241 feet of the vertisols boundary are scored 17, and all other areas are scored 0. Details of the soil scoring are provided in Table 6.

Table 6. Susceptibility scoring for mapped vertisols.

Criteria	**Number of slides**	**Percent of slides**	**Susceptibility Score**
Predominantly or completely within mapped vertisols boundary	6	85.7	100
0-241 feet of the mapped vertisols boundary	1	14.2	17
>241 feet from mapped vertisols boundary	0	0	0
NoData	--	--	0

Maps of alluvium and vertisols were combined in Figures 4 and 5. In general, there is a much greater area of mapped alluvium than of mapped vertisols. Most of the vertisols overlap with alluvium, but there are appreciable areas where there is no overlap. All seven studied slides are within or very near to areas of overlap.

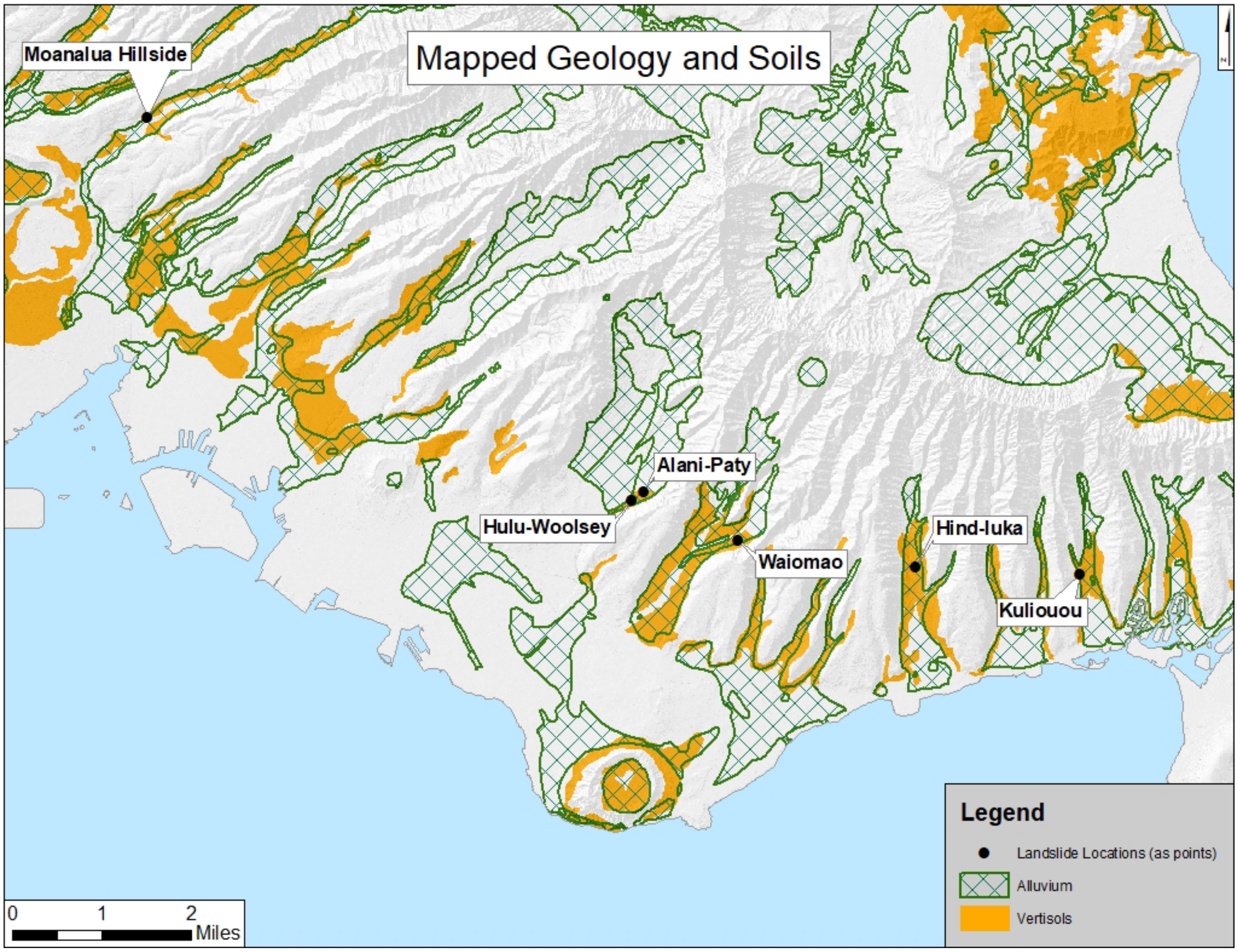

Figure 4. Mapped alluvium and vertisols in southeast O‘ahu.

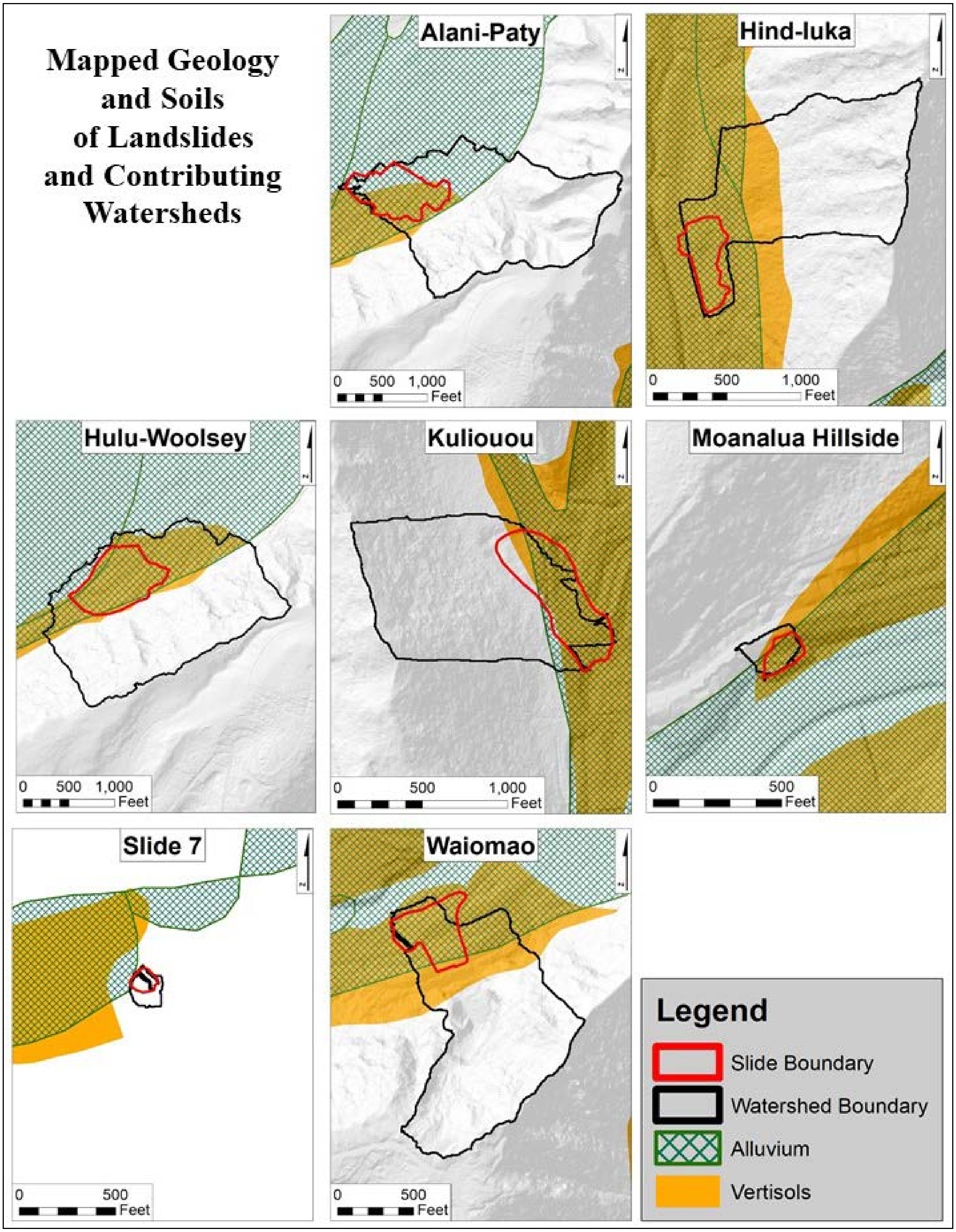

Figure 5. Mapped alluvium and vertisols at each of the seven studied slow-moving landslides.

3.2.2 Slope

We produced a slope raster in ArcMap using a 1-meter resolution DEM (Table 3). Slopes in southeast O‘ahu and in each of the analyzed landslide areas are shown in Figures 6 and 7, respectively. In accordance with the findings of *Ellen et al.* [1995], the landslides are in areas of low to moderate slopes, at the base of steeply sloping sides of the valleys.

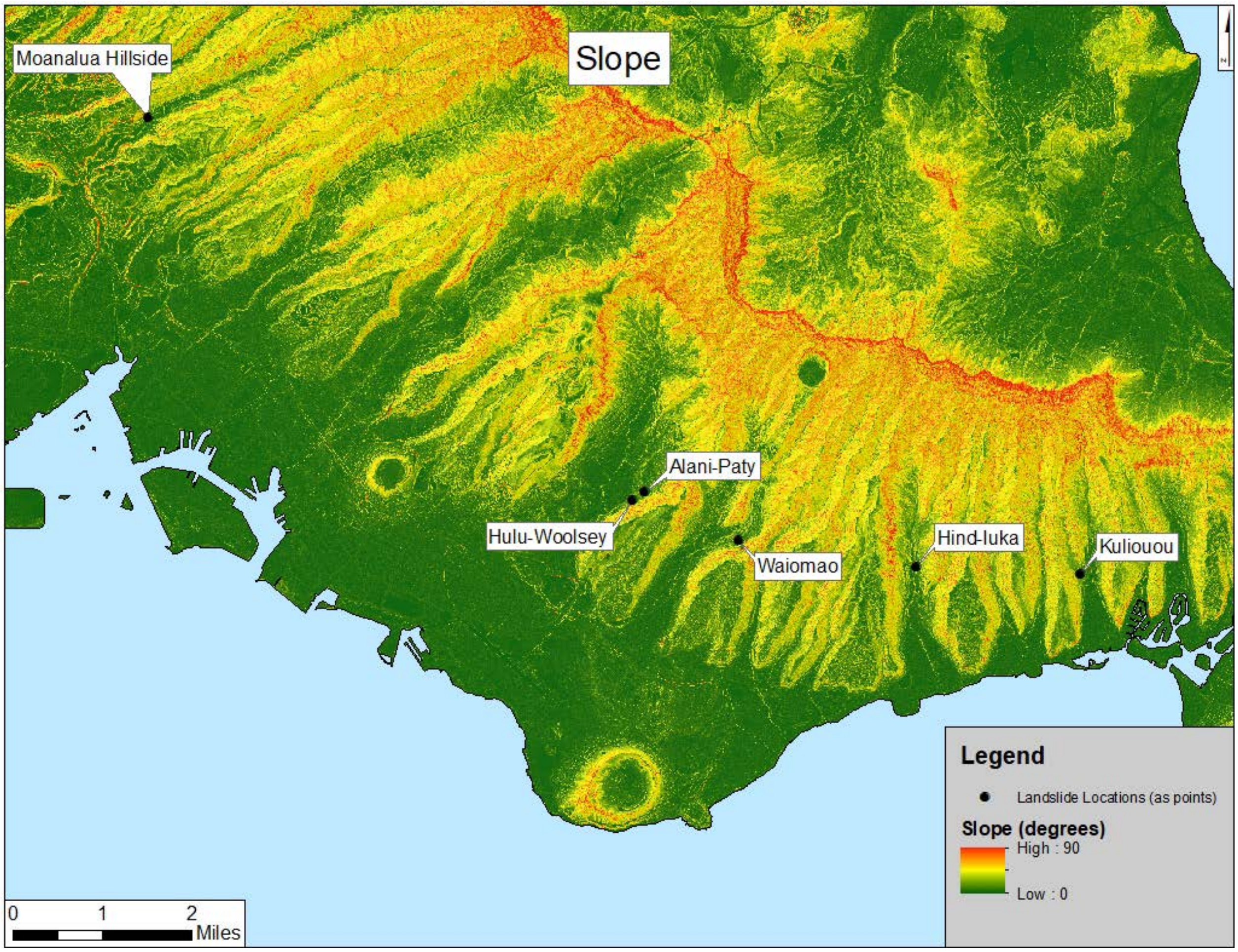

Figure 6. Slopes in southeast O‘ahu.

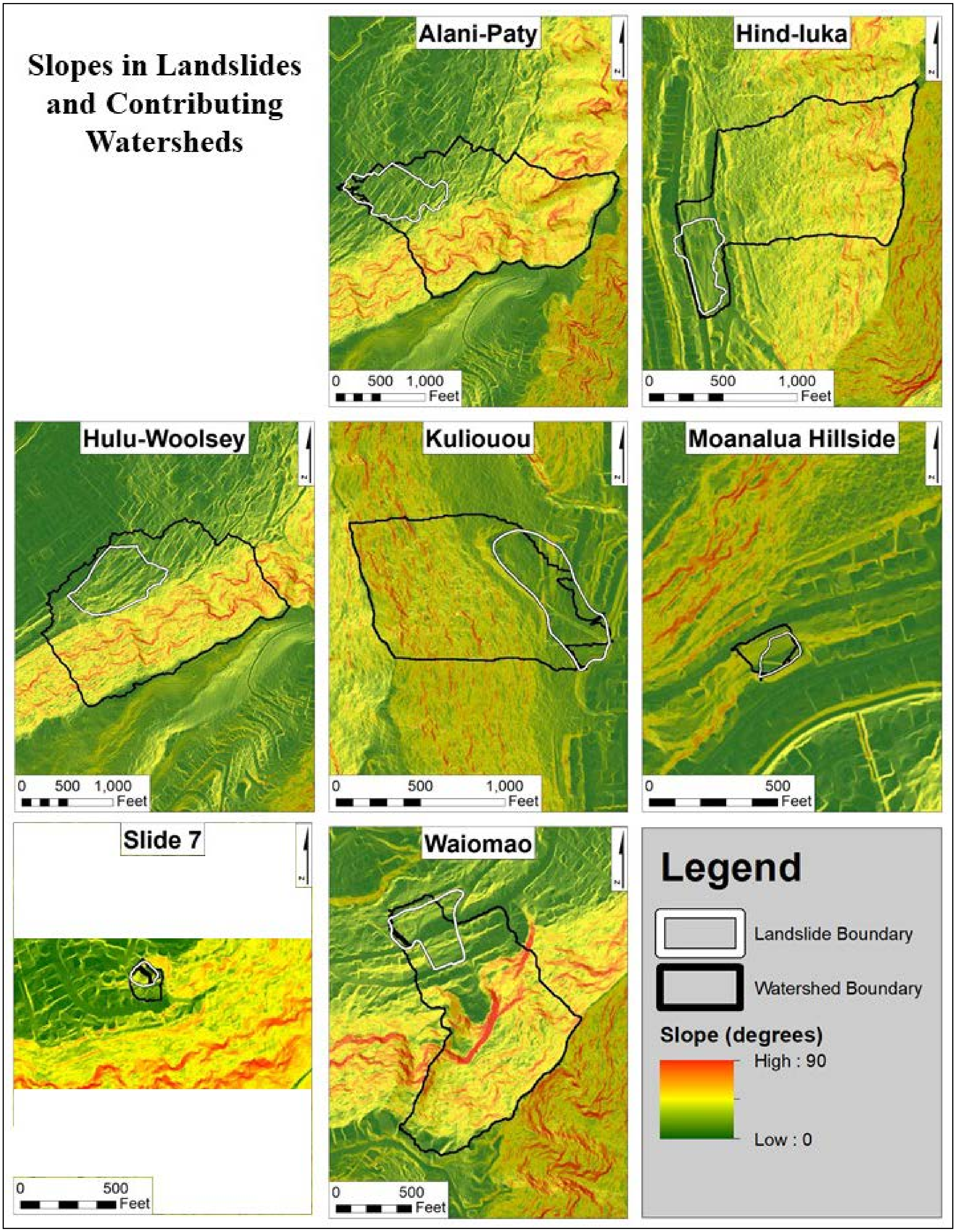

Figure 7. Slopes at each of the seven studied slow-moving landslides.

We exported the slope data from ArcMap, converted them to ASCII format, and analyzed them in MATLAB. For each of the slides, we computed and displayed probability density functions (PDFs) of slope angles using histograms of 100 bins each. We used the same process for each watershed and each valley, to assess if the slopes within a slide area reflected the watershed and/or the entire valley. The valleys generally show a bimodal distribution, with one peak at a very low slope (<~3°), reflecting the valley floor, and another peak at roughly 40°, representing the steep upper walls. Some of the landslide watersheds show a similar distribution, but with less pronounced peaks, and the upper peak generally between 30° and 35°; but others have more of a single-peaked distribution. Four of the slides have a distribution with a single peak whereas three others have two discernible peaks (Figure 8). Four slides have median slopes between 10° and 15°, and one has a median slope < 10° (Figure 8). The Moanalua Hillside has a strong bimodal distribution with peaks around 4° and 22° and a median of 18.2°; and Slide 7 has a broad single-peaked distribution with a median of 23.1°.

We then combined the 100-bin histograms to produce a single histogram characterizing all the slides together. To avoid having larger slides dominate the distribution, we drew 5 x 10^6 random samples from the PDF of each slide and combined all seven such samples to estimate the PDF of all the slides together (Figure 8). This technique caused each slide to contribute the same number of (random) samples. Running the random sampling multiple times showed negligible variation of final distribution.

Using this method, the median slope of all the slides together is 13.3°. In order to assign scores for different slope ranges, we created a PDF with 10 bins using the natural log of slope, a common practice when analyzing data that are limited to positive values. As shown in Figure 8 (bottom right), a comparison with the 100-bin PDF shows that the 10-bin PDF based on log (slope) provides reasonable approximation to the PDF; it was proven to be a much better approximation than a 10-bin PDF that did not use a log scale. We scaled the probability of each of the 10 slope bins so that the maximum equals a susceptibility score of 100. The resulting data are presented in Table 7, along with the scores.

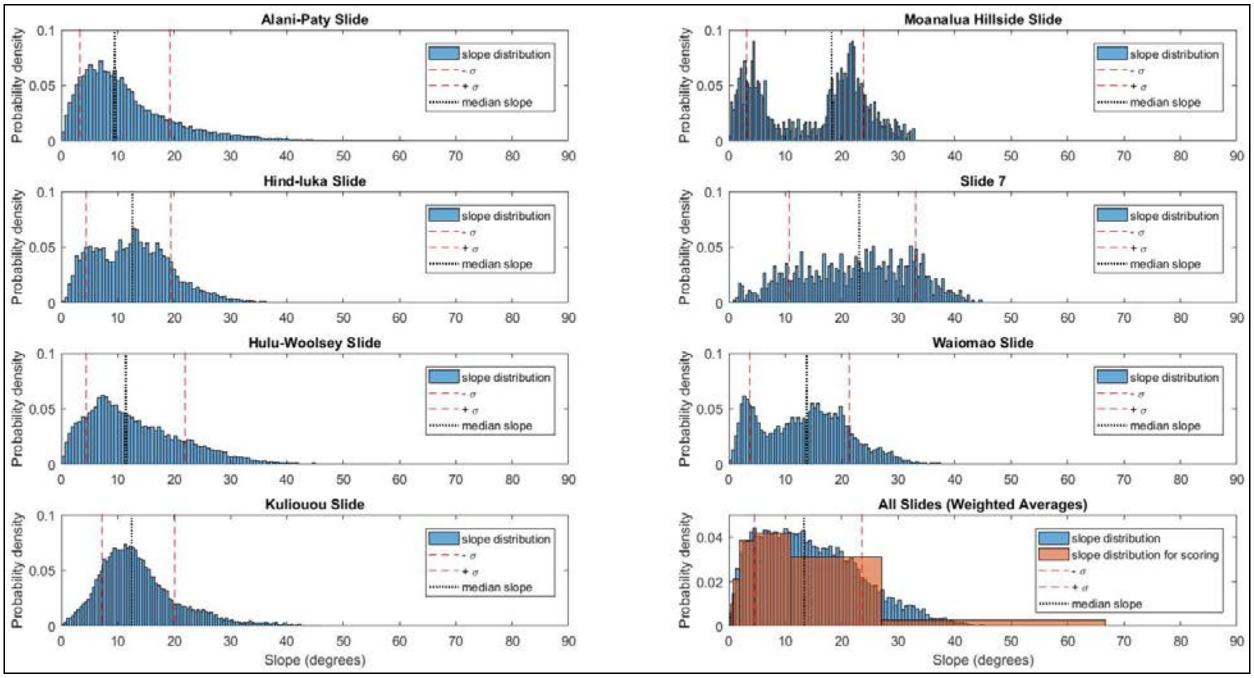

Figure 8**. Slope histograms for each slide individually as well as the combined distribution, labeled "All Slides".**
Note that the "All Slides" histogram has a different vertical scale from the individual slides. In a PDF, the area of each bar is proportional to the probability.

Table 7. Data from 10-bin PDF of log of slope, with resulting "susceptibility scores".

Slope (degrees)	Probability in each slope range (i.e. each histogram bin)	Scaled value (scaled to 100)	Susceptibility score
0 - 0.008	0.000	0.000	0
0.008 - 0.020	0.000	0.001	0
0.020 - 0.050	0.000	0.002	0
0.050 - 0.123	0.000	0.011	0
0.123 - 0.301	0.001	0.148	0
0.301 - 0.741	0.005	0.910	1
0.741 - 1.822	0.023	4.583	5
1.822 - 4.482	0.102	20.518	21
4.482 - 11.023	0.273	54.950	55
11.023 - 27.113	0.497	100.000	100
27.113 - 66.686	0.099	19.846	20

Slope (degrees)	Probability in each slope range (i.e. each histogram bin)	Scaled value (scaled to 100)	Susceptibility score
66.686 - 90	0.000	0.000	0
NoData	--	--	NoData*

*A score of “NoData” means that in the weighted analyses, a cell that has NoData in any category will end up as NoData in the final output; that is, the cell will not be given a value.

3.2.3 Infiltration

Maps of infiltration are shown in Figures 9 and 10. Within the slides areas the medians range from 25.69 to 78.21 in/yr (Figure 11). We followed the same procedure as that used for slopes, by random sampling the PDFs of each slide and combining the seven samples to estimate the PDF of all slides together. The median of the combined population is 61.5 in/yr. For comparison, infiltration on the entire island ranges from 7.35 to 528.87 in/yr.

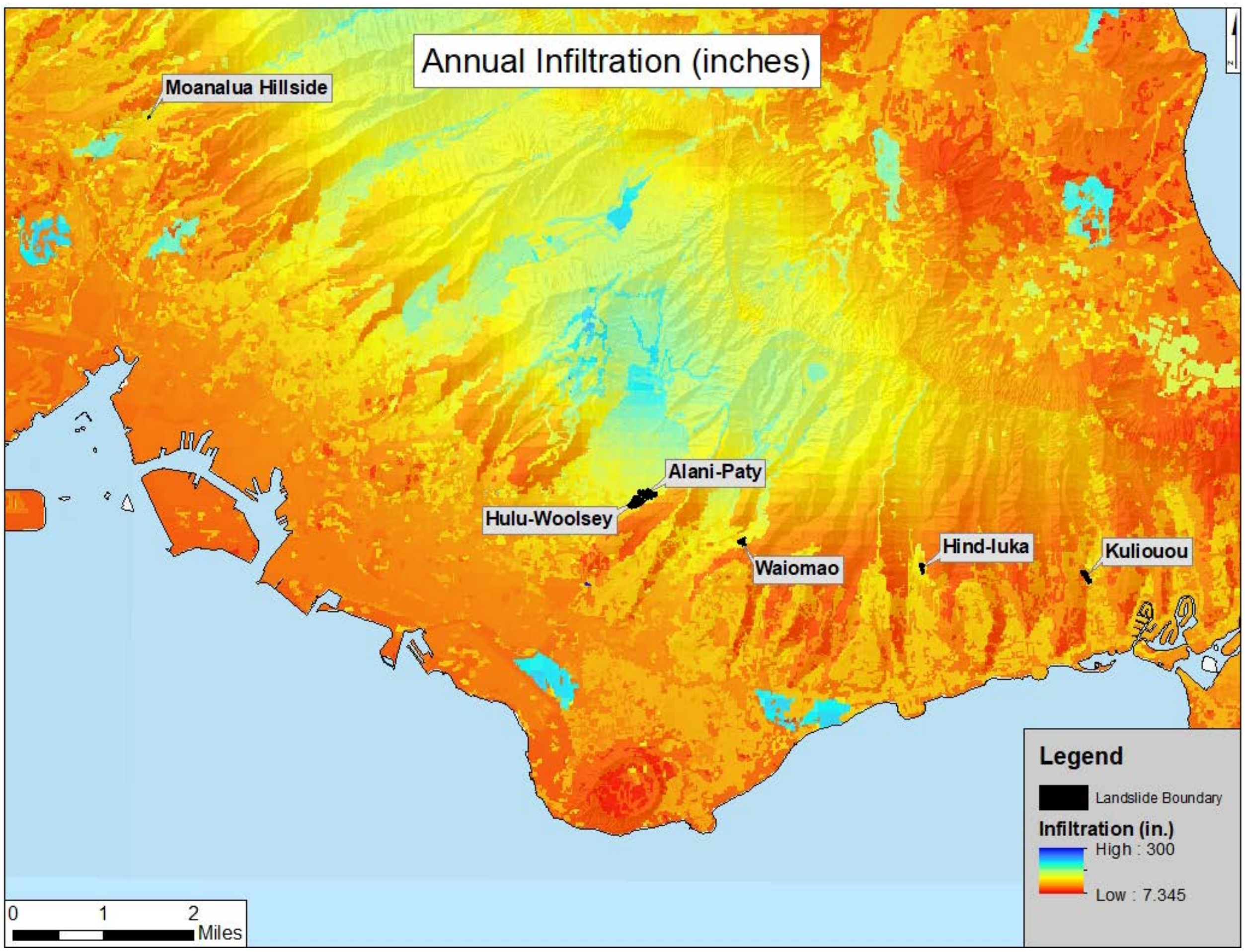

Figure 9. Annual infiltration in southeast O‘ahu.

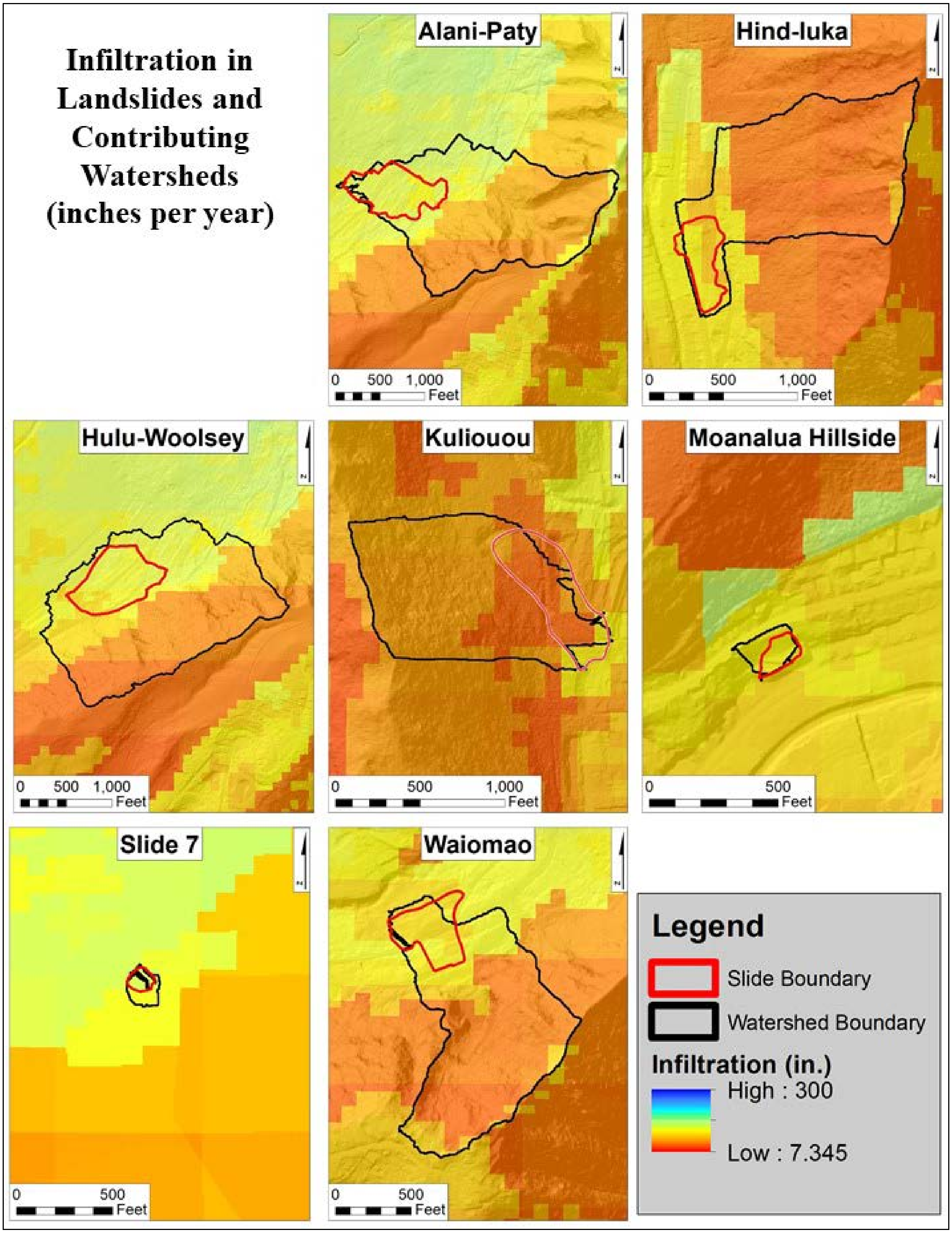

Figure 10. Infiltration at each of the seven studied slow-moving landslides.

We assigned susceptibility scores for different infiltration values following the same procedure we used for slope. We created a PDF with 10 bins, using log of infiltration (Figure 11), and scaled the number of values in each histogram bin so that the maximum equals a score of 100. The resulting data are presented in Table 8, along with the scores.

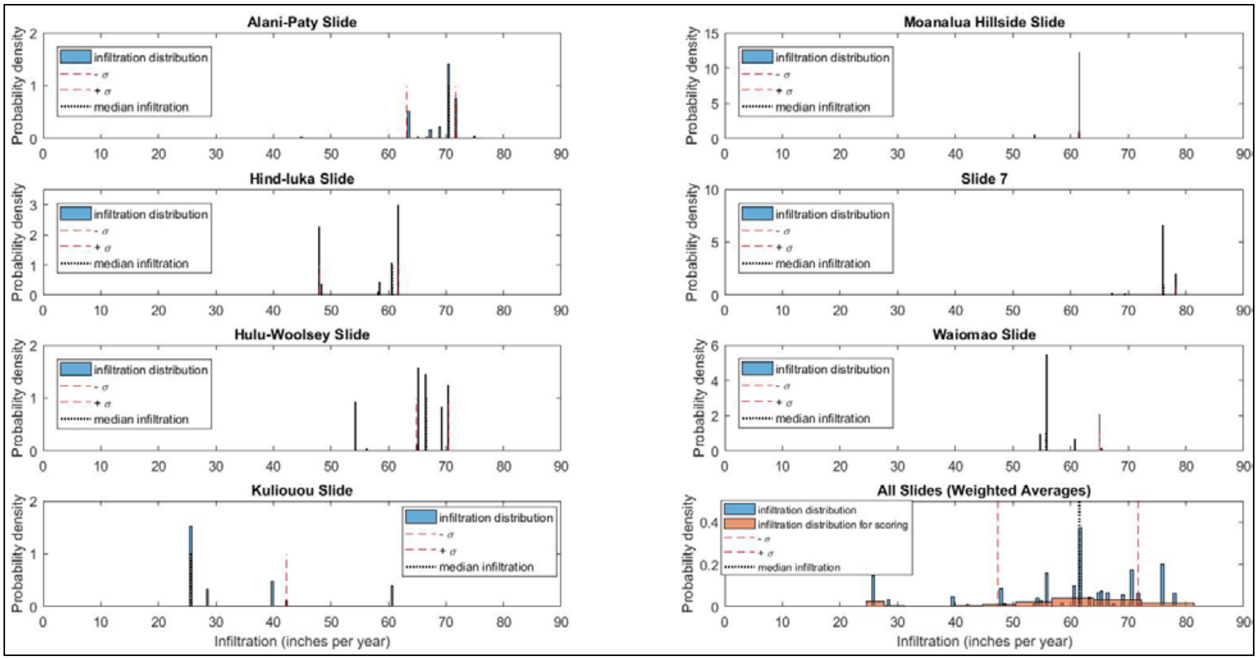

Figure 11**. Infiltration histograms. Note that vertical axes vary.**

Table 8. Data from 10-bin PDF of log of infiltration, with resulting “scores”.

Infiltration (inches per year)	Probability in each infiltration range (i.e. each histogram bin)	Scaled value (scaled to 100)	Susceptibility score
<7.345	--	--	NoData*
7.345 - 24.533	0.000	0.000	0
24.533 - 27.660	0.077	27.395	27
27.660 - 31.187	0.016	5.901	6
31.187 - 35.163	0.000	0.000	0
35.163 - 39.646	0.000	0.000	0
39.646 - 44.701	0.030	10.822	11
44.701 - 50.400	0.054	19.186	19
50.400 - 56.826	0.127	45.316	45

Infiltration (inches per year)	**Probability in each infiltration range (i.e. each histogram bin)**	**Scaled value (scaled to 100)**	**Susceptibility score**
56.826 - 64.072	0.280	100.000	100
64.072 -72.240	0.276	98.709	99
72.240 - 81.451	0.141	50.290	50
81.451 – 528.87	0.000	0.000	0
NoData	--	--	NoData*

*A score of “NoData” means that in the weighted analyses, a cell that has NoData in any category will end up as NoData in the final output; that is, the cell will not be given a value.

3.2.4 Aspect

Five of the studied slow-moving landslides are on the east side of the valley, and two, Kuliouou and Moanalua Hillside, are on the west side. It has been hypothesized that strong afternoon sun, which the east sides of the valleys receive, promotes more vigorous a drying-and-wetting cycles that facilitate development of vertisols. Although we are unaware of any studies that examine this correlation, we decided to analyze aspect – the compass direction that the downhill slope faces – as a possible factor in these types of landslides. Maps of aspect are shown in Figures 12 and 13.

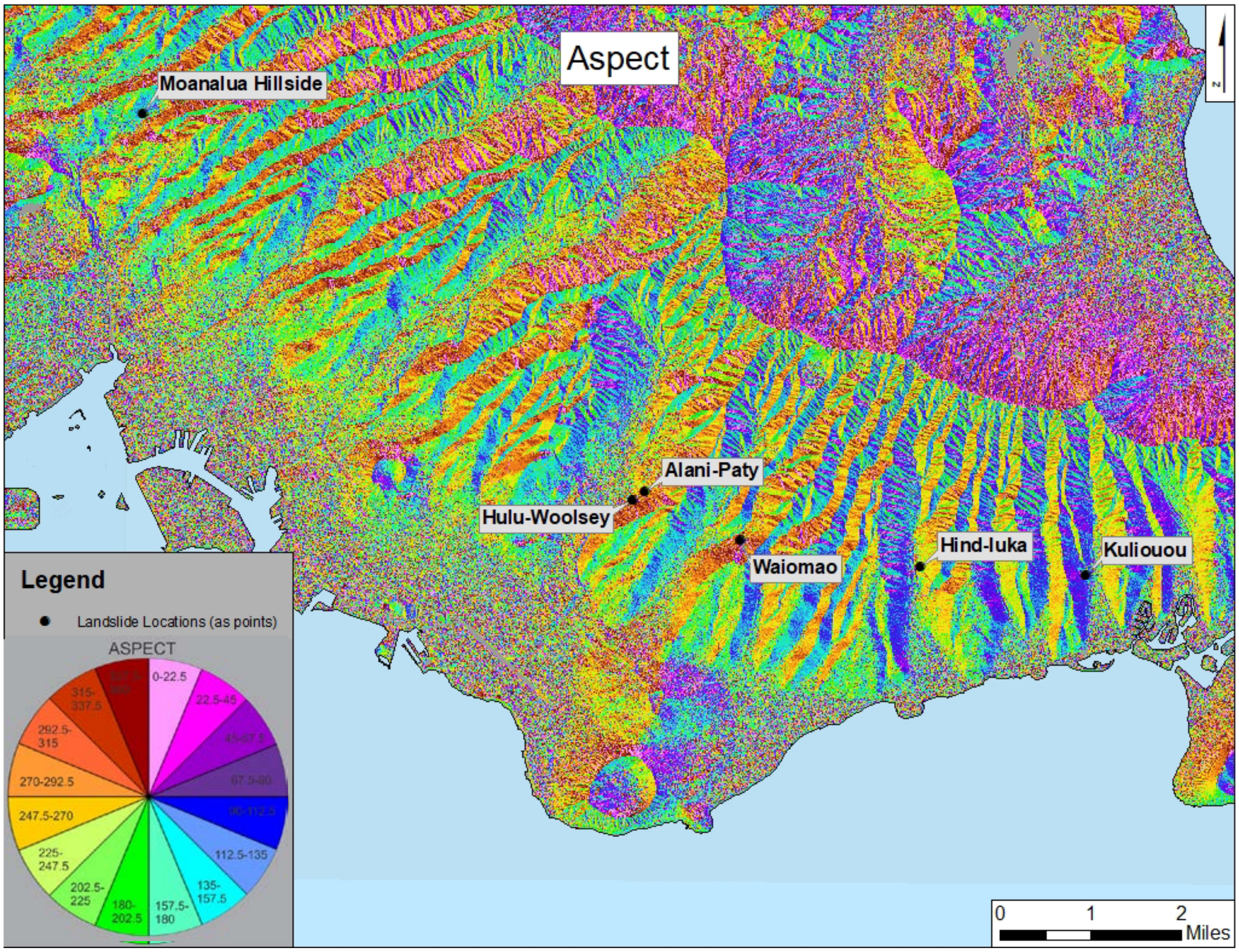

Figure 12. Aspect in southeast O‘ahu.

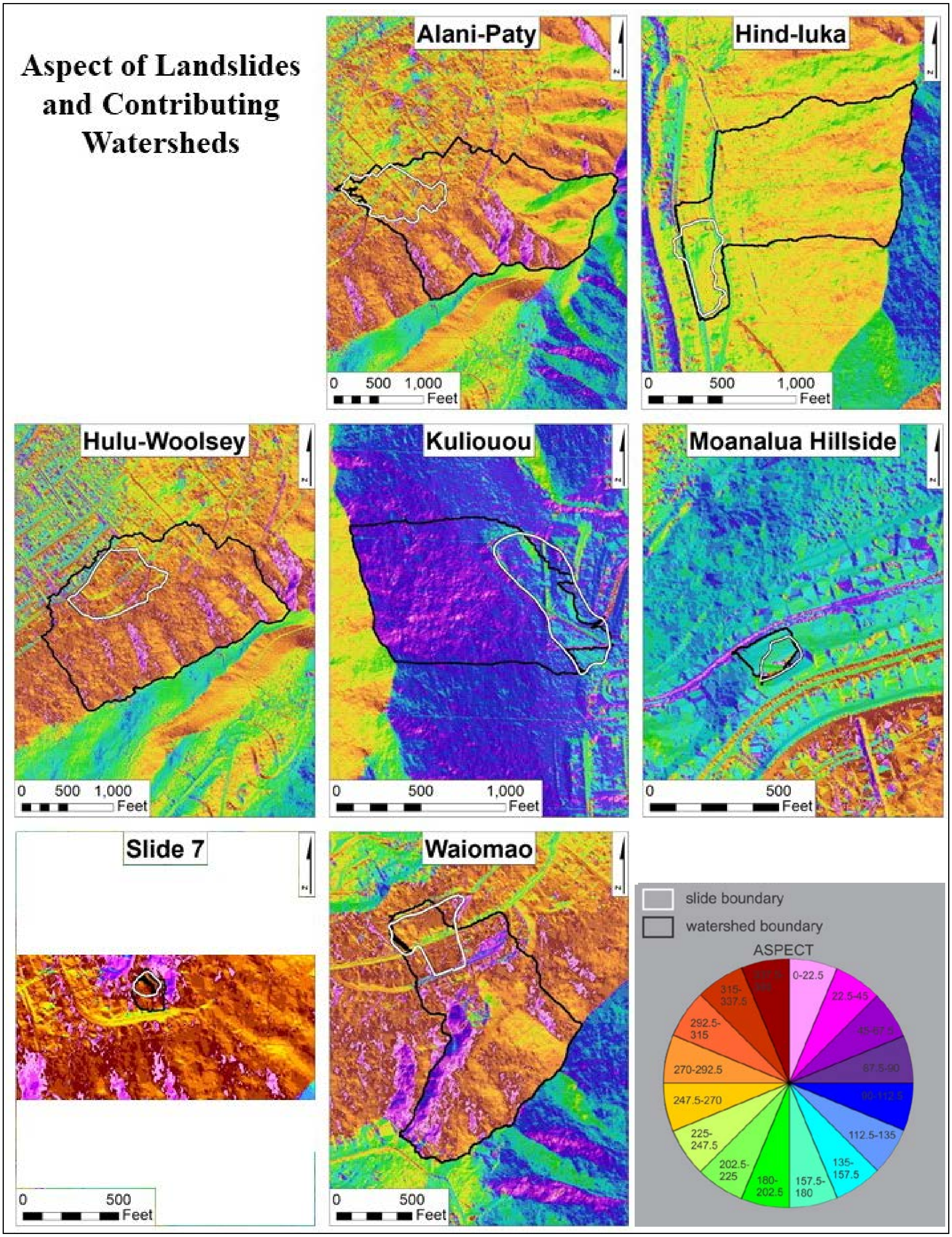

Figure 13. Aspect at each of the seven studied slow-moving landslides.

Within the slide areas of Kuliouou and Moanalua Hillside, on the west side of the valley, median aspects are 113.3° and 159.3°, respectively. The medians of the other five slides, on the east sides of valleys, range from 240.4 to 325.2° (Figure 14). Again we randomly sampled the PDFs of each slide and combined the seven samples to estimate the PDF of all slides together. The median of the combined population is 265.3°.

For the 10-bin histogram used for scoring, we did NOT use a logarithmic scale for aspect because aspect can be both positive and negative: Flat areas are assigned an aspect between -1 and 0. Susceptibility scoring is presented in Table 9.

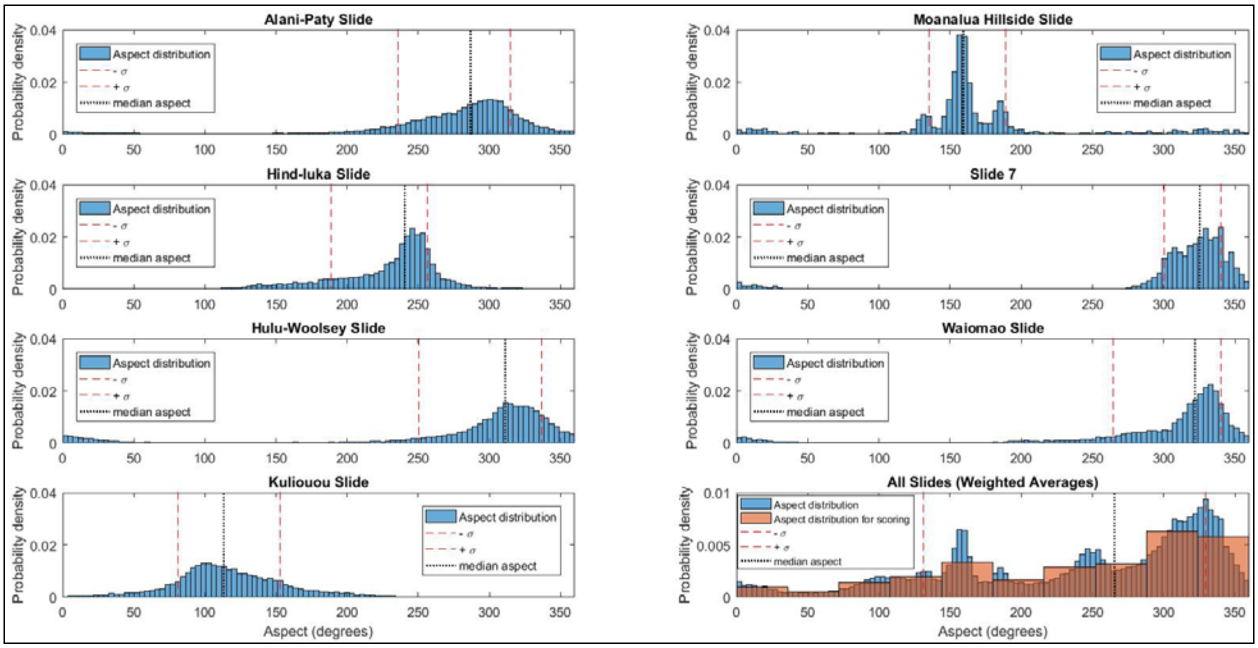

Figure 14**. Aspect histograms.**
Note that the "All Slides" histogram is on a different vertical scale from the individual slides.

Table 9. Data from 10-bin PDF of aspect, with resulting "scores".

Aspect (degrees)	Probability each aspect range (i.e. each histogram bin)	Scaled value (scaled to 100)	Susceptibility score
< 0 (flat)	0.000	0.000	0
0 - 36	0.033	14.548	15
36 -72	0.017	7.461	7
72 - 108	0.052	23.019	26
108 - 144	0.070	30.838	31

Aspect (degrees)	Probability each aspect range (i.e. each histogram bin)	Scaled value (scaled to 100)	Susceptibility score
144 - 180	0.119	52.556	53
180 - 216	0.060	26.517	27
216 - 252	0.102	44.929	45
252 - 288	0.113	49.974	50
288 - 324	0.227	100.000	100
324- 360	0.207	91.092	91
NoData	--	--	NoData

3.2.5 Solar Radiation

The dataset of solar radiation that we analyzed is in hourly W/m^2 averaged over a year, and the spatial resolution of the dataset is 250 m (Figure 15). In a similar fashion to the susceptibility scoring for soils and geology, we based the susceptibility scoring of solar radiation on the percent of slides that was in a specific range of solar radiation, as shown in Table 10. The selection of ranges was somewhat arbitrary: a range of 180 to 210 W/m^2 could have been selected and assigned a score of 100, with everything else receiving a score of 0. However, because it appeared that each slide was more or less in a distinct range, we decided to use multiple ranges. Susceptibility scores were scaled to a maximum of 100.

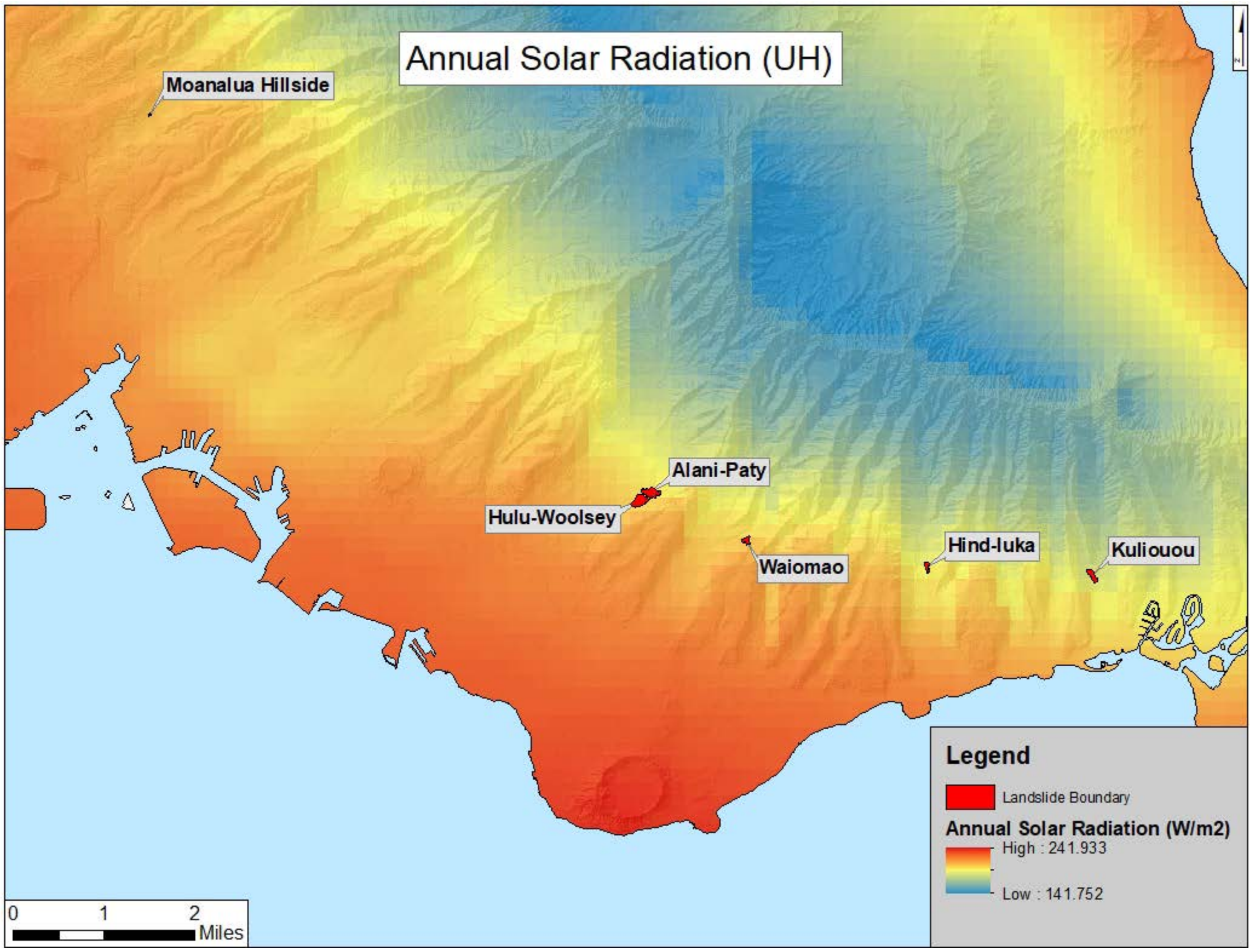

Figure 15. Annual solar radiation in southeast O‘ahu.

Table 10. Scoring of solar radiation ranges.

Solar radiation (W/m^2)	Number of slides	Percent of slides	Susceptibility score
< 180	0	0	0
180-185	1	14.3	29
185-195	1.5	21.4	43
195-205	3.5	50	100
205-210	1	14.3	29
>210	0	0	0
NoData	--	--	0

3.2.6 Elevation

Although elevation in southeast O‘ahu ranges from 0 to 3160 feet (Figure 16), all seven of the studied slow-moving landslides are completely within the elevation range of 80 to 440 feet (Figure 17). The elevation range of the head scarps is 235 to 440 feet, and the elevation range of the toes of the slides is 80 to 360 feet. The elevation change within slides varies from 45 to 210 feet (Figure 18). This variation made it difficult to set specific elevation ranges for scoring. Therefore, we set a single range of elevations in which all seven slides fall, resulting in scoring as presented in Table 11.

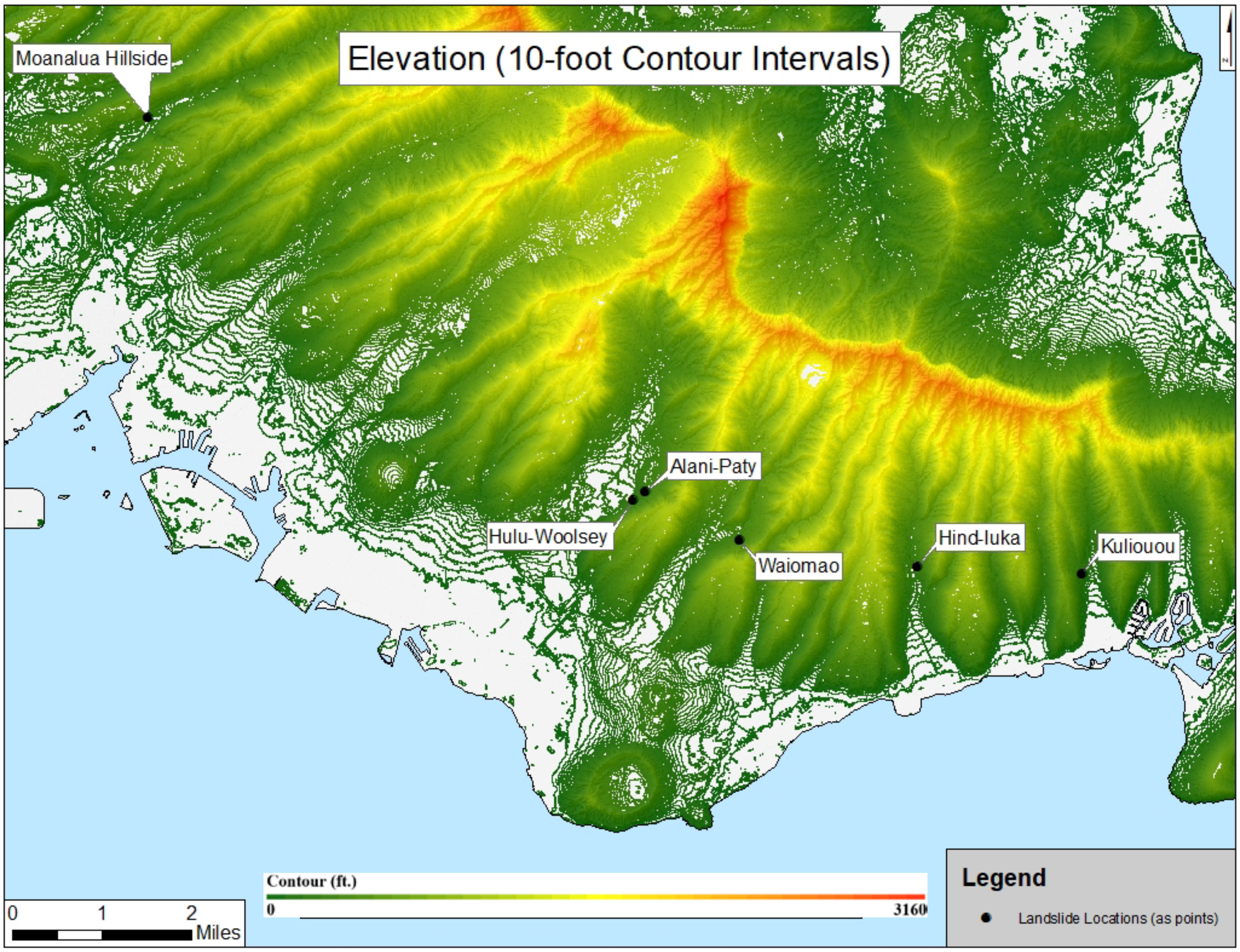

Figure 16. Elevation in southeast O‘ahu.

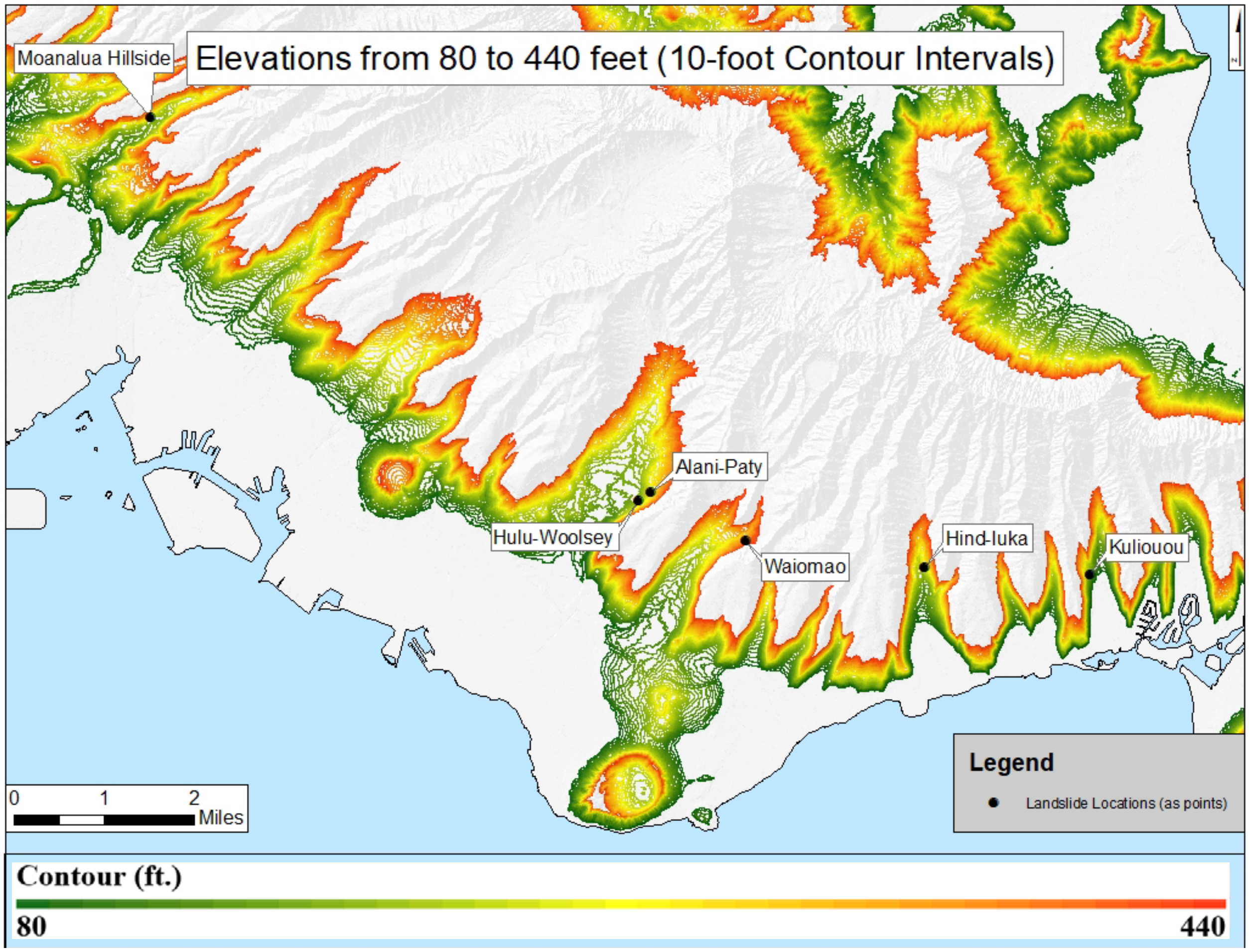

Figure 17. Elevation range from 80 to 440 feet in southeast O‘ahu.

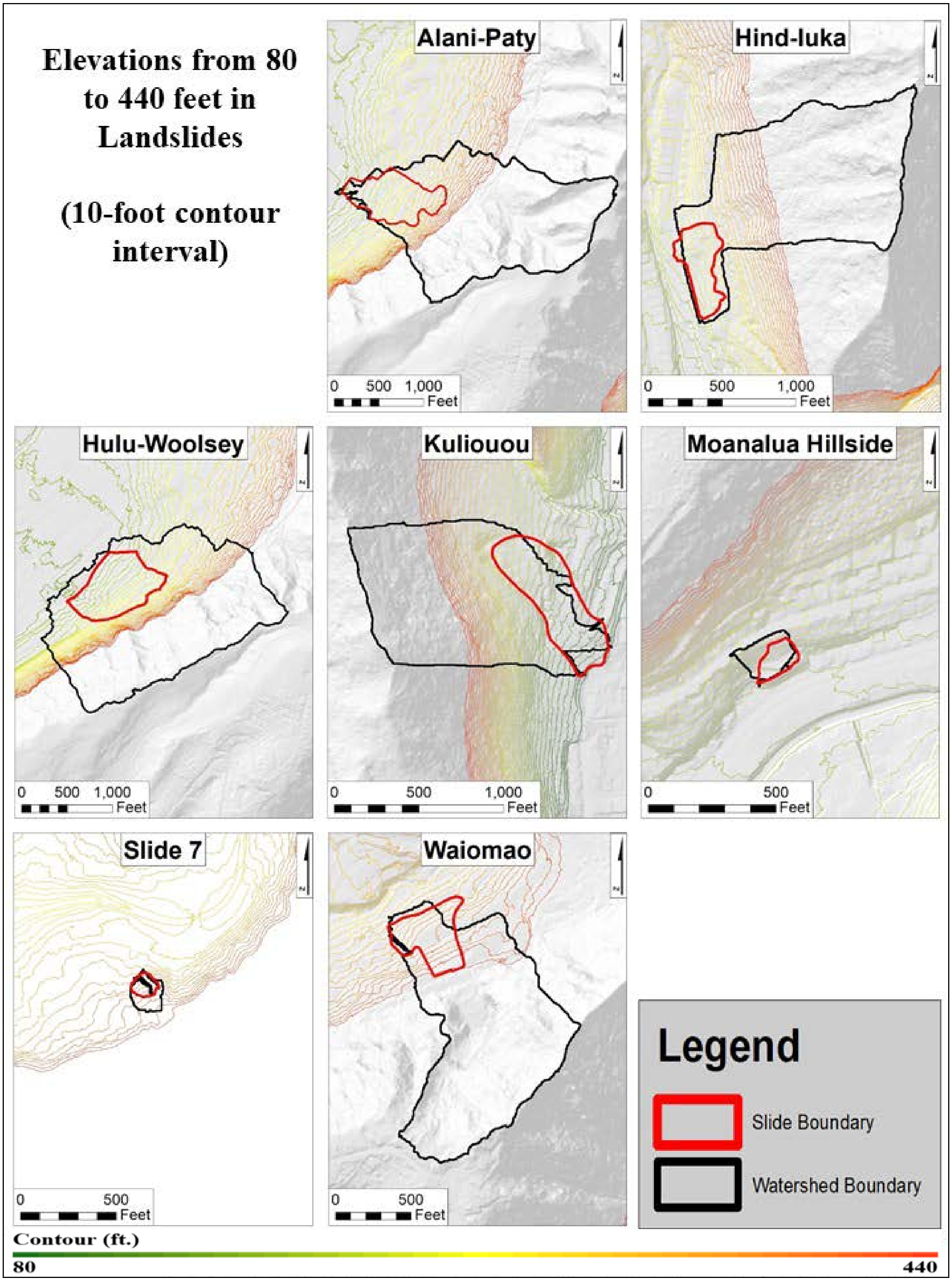

Figure 18. Elevation range from 80 to 440 feet in each of the seven studied slow-moving landslides. Elevations are colored as indicated by the color bar below and contoured every10 feet.

Table 11. Scoring of elevation.

Elevation (feet)	Number of slides	Percent of slides	Susceptibility score
< 80	0	0	0
80-440	7	100	100
>440	0	0	0
NoData	--	--	0

4.0 SUSCEPTIBILITY MAPS

4.1 Weighting the Susceptibility Parameters

To combine the effects of the seven selected susceptibility parameters that have been quantified, we assigned a weight to each parameter. This weighting is important because some parameters likely influence susceptibility to slow-moving landslides more than others. For example, there is no proposed mechanism for elevation to affect susceptibility except as it influences rainfall, in which case it is spatially redundant with infiltration (which depends on rainfall). Secondly, some of the parameters are likely to be interdependent. For example, the development of vertisols may be related to infiltration, aspect, and solar radiation. In order to attempt to assess how different parameters may influence the final mapping, we made several maps, first with only two parameters, and then with additional parameters. Analysis maps are presented as Figures 19 through 22.

We proceeded using two approaches. In the first approach, we weighted all seven factors equally (Figure 23). Weights are recorded as percentages, with the weights of all parameters totaling 100. In the second approach, weights were defined using a method often used in knowledge-driven assessments like this, called “expert elicitation” [e.g., *O’Hagan et al.* 2006; *O’Leary et al.* 2009]. Here, four experts were asked to provide weights representing their opinions about the importance of the seven selected parameters to the susceptibility of slow-moving landslides, based on their knowledge and experience. We weighted the recommendation for each expert by a factor based on his or her experience, with the most experienced expert’s weights carrying twice the weight of each of the others (Figure 24).

The susceptibility maps display the “Sum of weighted scores”, which was calculated using the Spatial Analyst >Map Algebra > Raster Calculator function in ArcMap. The score for each parameter in a given map cell is multiplied by the parameter’s weight as a percentage (with the total weights equaling 100), and the weighted scores are then summed. A high sum of weighted scores represents high susceptibility to slow-moving landslides, and a low sum of weighted scores represents low susceptibility. For example, if slope and aspect are the only parameters considered and are weighted equally, the formula for the weighted scores would be (slope x 0.5) + (aspect x 0.5). The Raster calculator did not function for decimals beyond hundredths; therefore, even though Figure 23 indicates that the parameters are weighted equally, two of them are actually weighted 15 percent each, and the other five parameters are each weighted 14 percent. The raster cell size was set at 3.2808 feet (1 meter) in order to preserve the resolution of the data layers that were produced at that resolution. This results in an artificially high resolution for data mapped at a larger scale, such as the solar radiation.

4.2 Susceptibility Maps

Before creating the two final susceptibility maps, which include all seven parameters, we first examined the effects of individual factors on susceptibility. Figure 19 shows the effects of only two parameters, slope and aspect. The areas with high susceptibility (red zones) are distributed in patches of relatively small area, and in general, occur at west-facing slopes near the base of steeper slopes. Areas of low susceptibility (blue zones) are on steep slopes, valley floors, and slopes facing north and east. Figure 20 displays the effects of alluvium and vertisols alone. The overlap of the two parameters is largely near the base of slopes, on portions of valley floors, in some but not all craters, and in a few other areas. Figure 21 presents the effects of vertisols and slope. Areas of high susceptibility are generally larger and more contiguous than in the map considering only the slope and aspect, and are smaller and less contiguous than in the map considering only alluvium and vertisols. Figure 22 presents an analysis of four parameters – alluvium, vertisols, slope, and aspect – weighted equally. The areas with a high susceptibility are much smaller than in the preceding maps with alluvium and vertisols, and slope and vertisols; but larger than the map with slope and aspect.

Figure 23 presents an analysis of all seven parameters weighted equally. Figure 24 presents the analysis based on Expert Elicitation. A visual comparison of these two susceptibility maps indicates that equal weighting results in slightly larger areas of high susceptibility (shown in red) and significantly larger areas of intermediate susceptibility (orange and yellow), which includes valley floors.

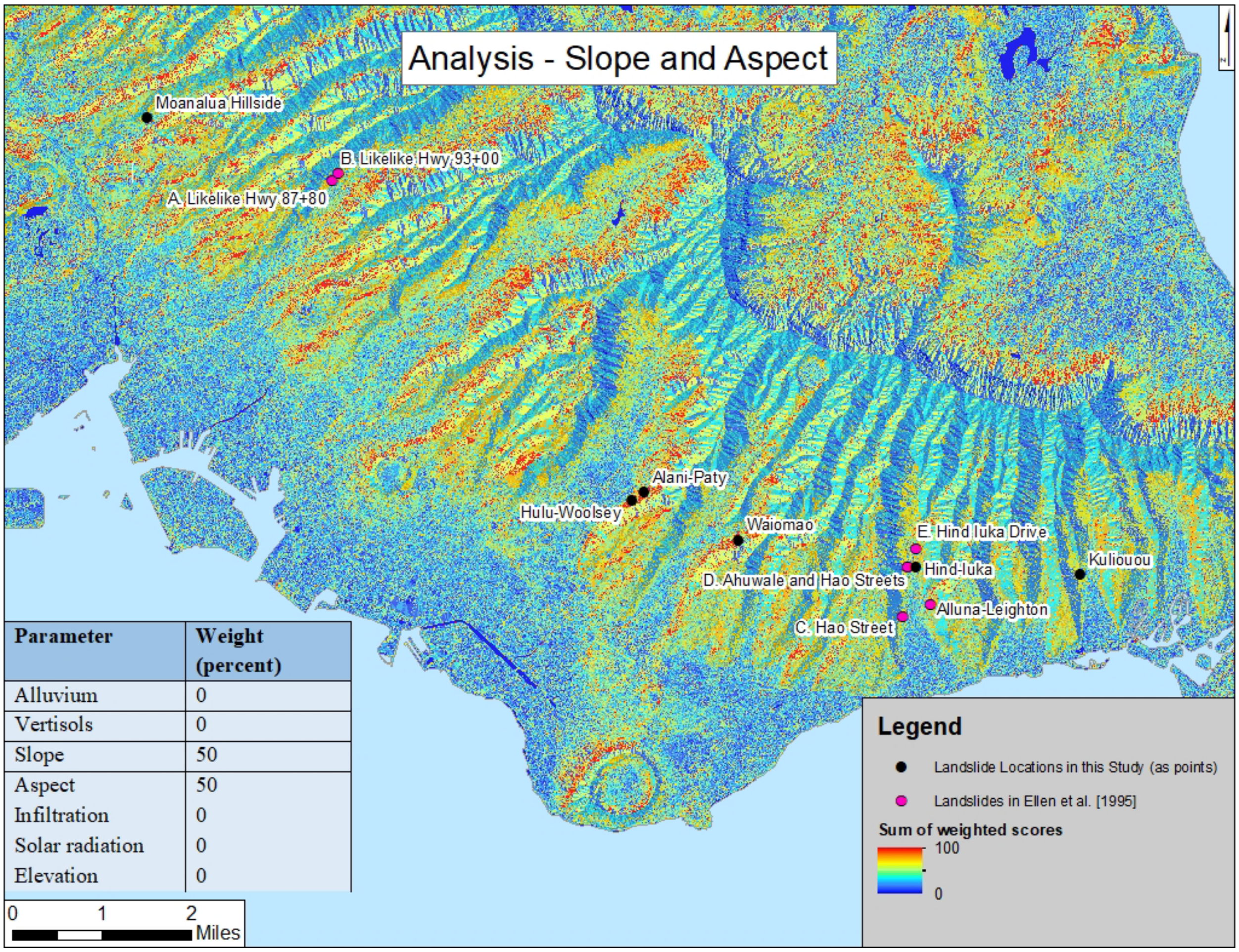

Figure 19. Analysis of two parameters, weighted equally: slope and aspect.

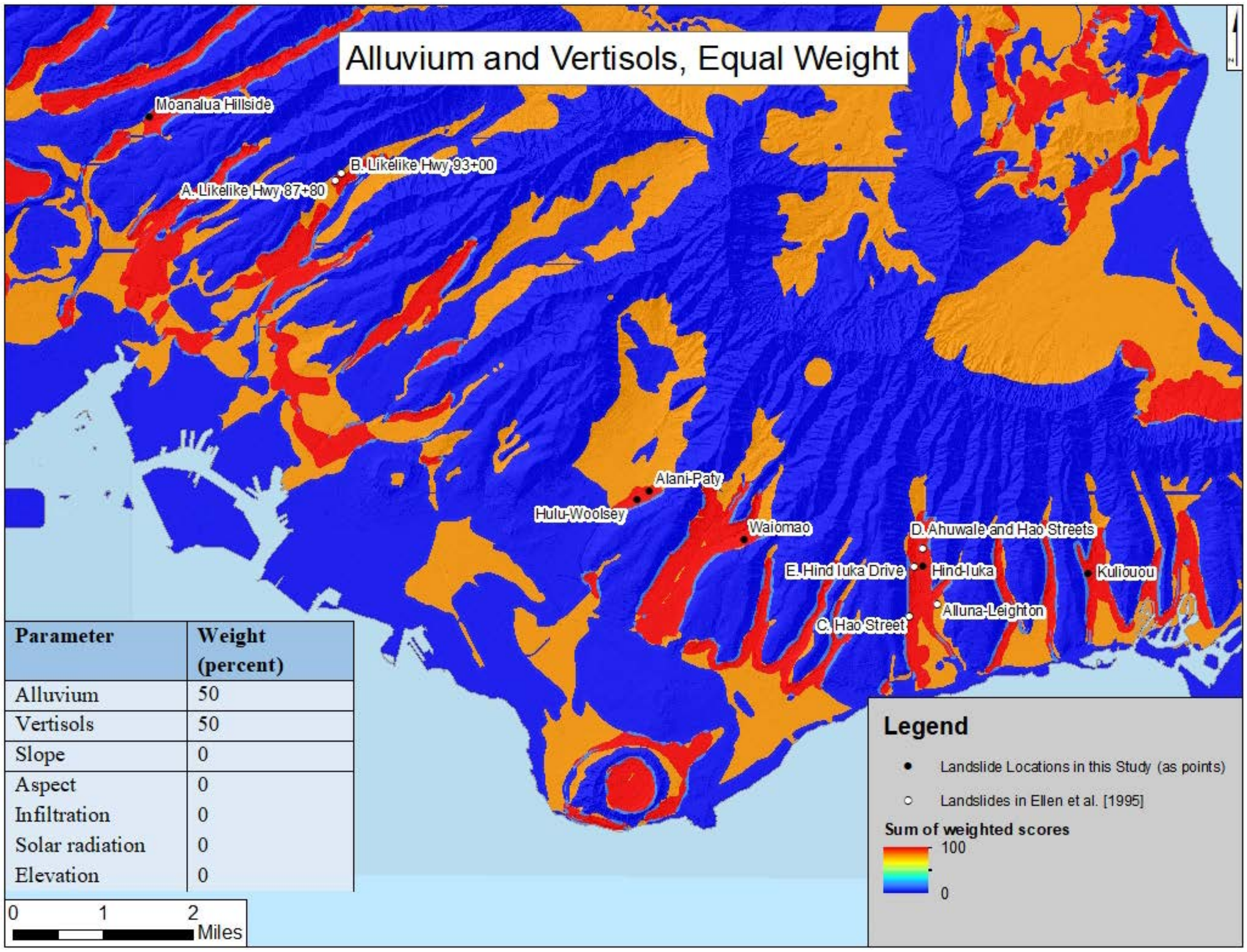

Figure 20. Analysis of two parameters, weighted equally: alluvium and vertisols.

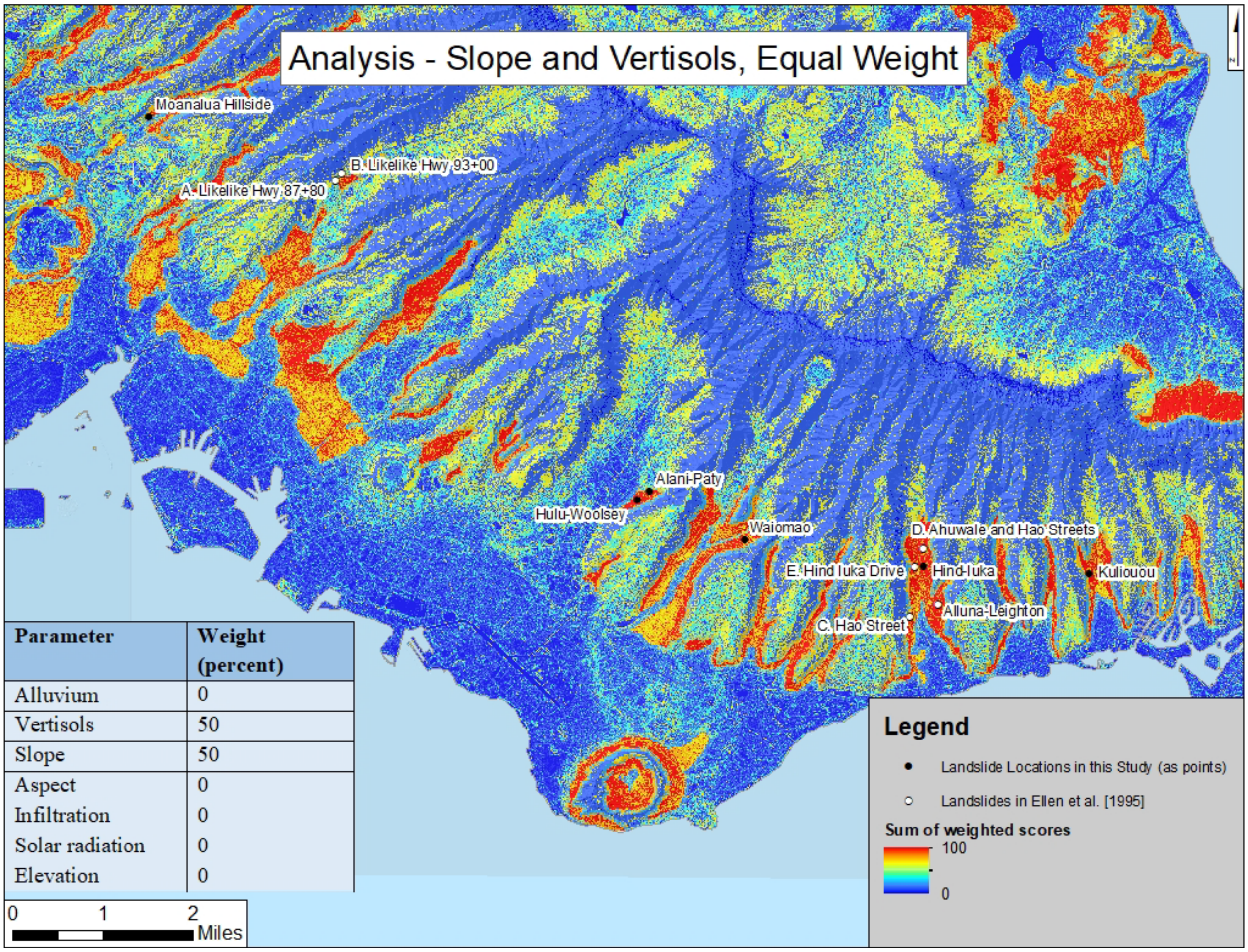

Parameter	Weight (percent)
Alluvium	0
Vertisols	50
Slope	50
Aspect	0
Infiltration	0
Solar radiation	0
Elevation	0

Figure 21. Analysis of two parameters, weighted equally: slope and vertisols.

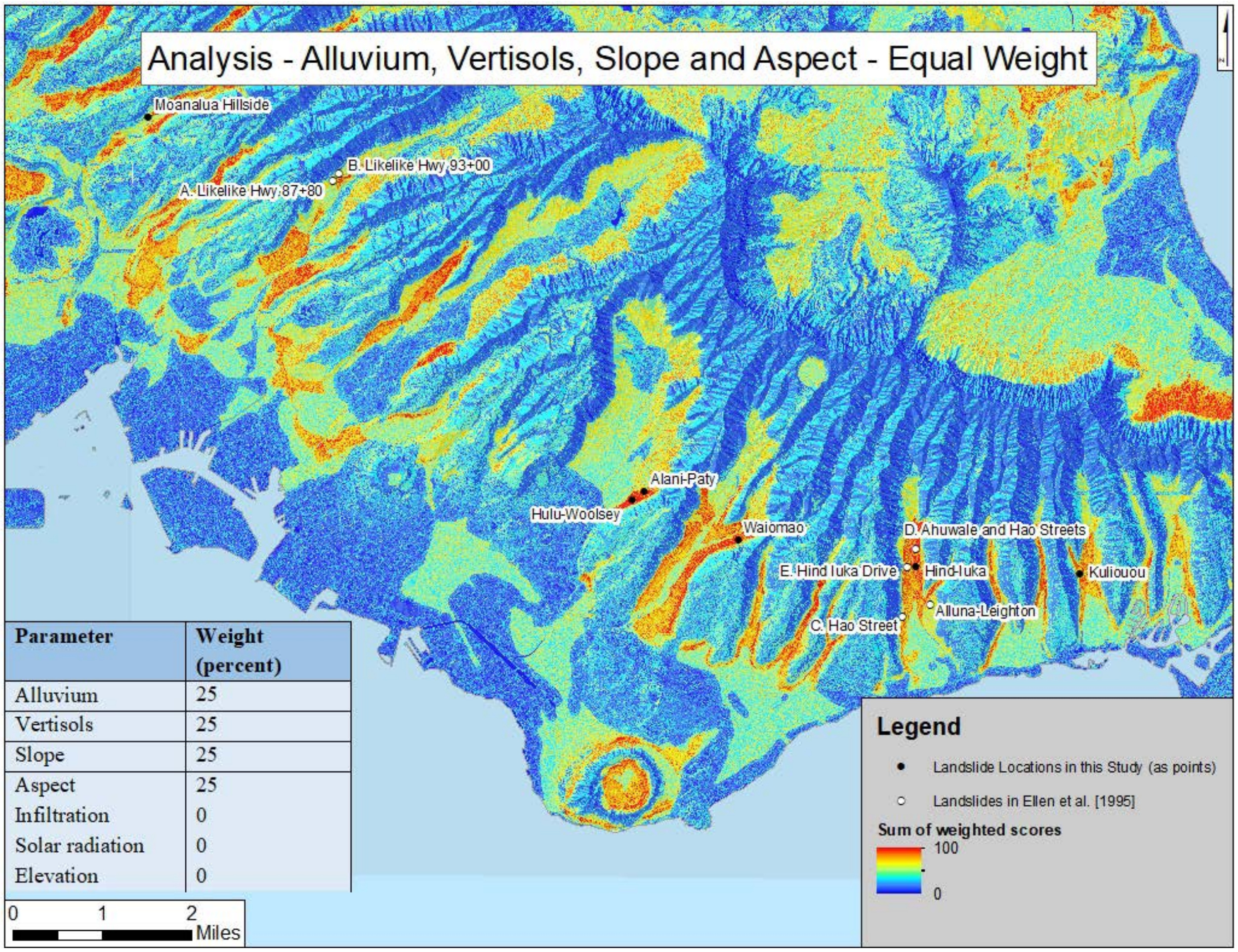

Figure 22. Analysis of four parameters, weighted equally: alluvium, vertisols, slope and aspect.

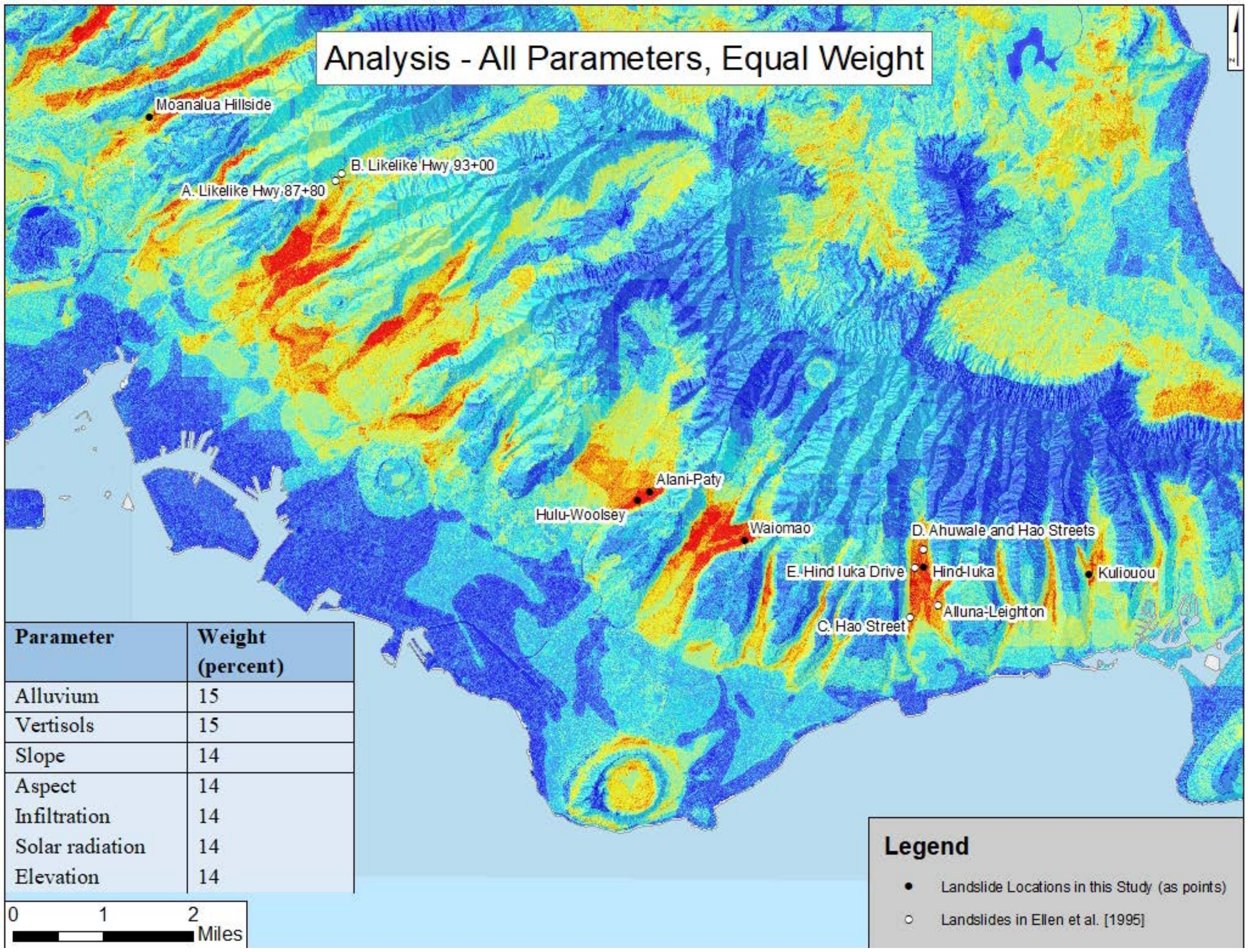

Figure 23. Susceptibility map, all parameters weighted equally.

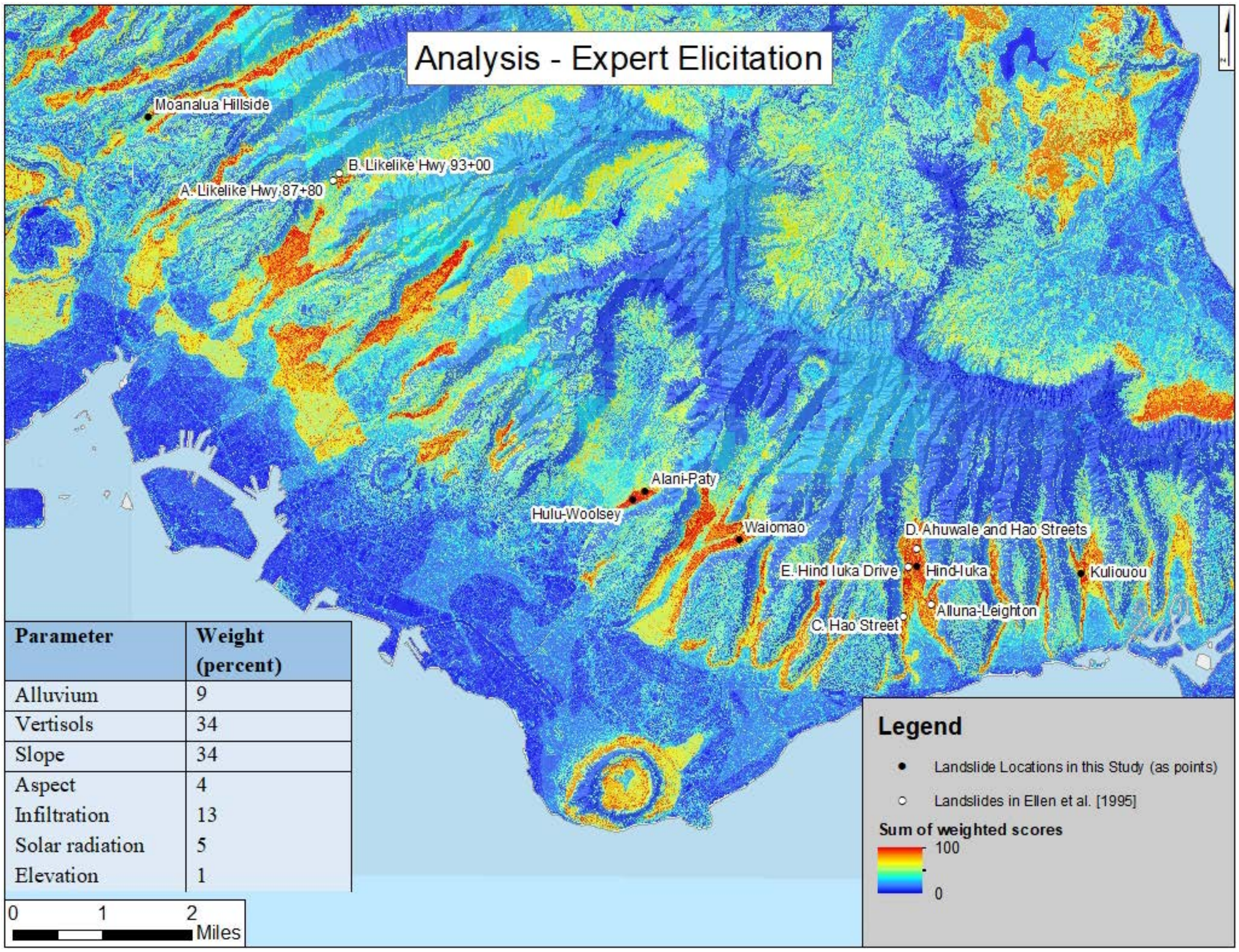

Figure 24. Susceptibility map, parameters weighted by expert elicitation.

4.3 Defining Low, Medium, and High Susceptibility

To define what sum of weighted scores should be considered low, medium, or high susceptibility, we examined the distributions of the weighted scores within the seven slides. Following creation of the two susceptibility maps that use all seven parameters, we clipped the landslide areas of the seven slides in our study from the two rasters that were produced using the Raster calculator (All parameters weighted equally, and Expert Elicitation). We produced PDFs in the same manner as we did for analysis of slope, infiltration, and aspect (Figures 25 and 26).

For the equal weight analysis, the median "sum of weighted scores" ranges from 62.5 to 92.3 among the seven slides individually, has a median of 79.0 for all the slides combined. For the combined distribution, the 15.9 and 84.1 percentiles (corresponding to ± 1 standard deviation σ about the mean for a normal distribution) are 64.8 and 92.0, respectively. For the expert elicitation analysis, the median "sum of weighted scores" ranges from 42.5 to 92.2 for the individual slides, and the slides have a combined median of 79.3. The 15.9 and 84.1 percentiles are 56.8 and 94.3, respectively.

For both analyses, the maximum "sum of weighted scores" within the combined slide areas is 100, but the minimum differs: in the equal weight analysis, it is 26.4, whereas in the expert elicitation analysis, it is 13.2. Table 12 illustrates the different medians of the "sums of weighted scores" for the two susceptibility maps. Based on the PDFs, we assigned categories to the "sums of weighted scores" as follows:

• ≥ median	High susceptibility
• 15.9 percentile to median	Medium susceptibility
• < 15.9 percentile	Low susceptibility

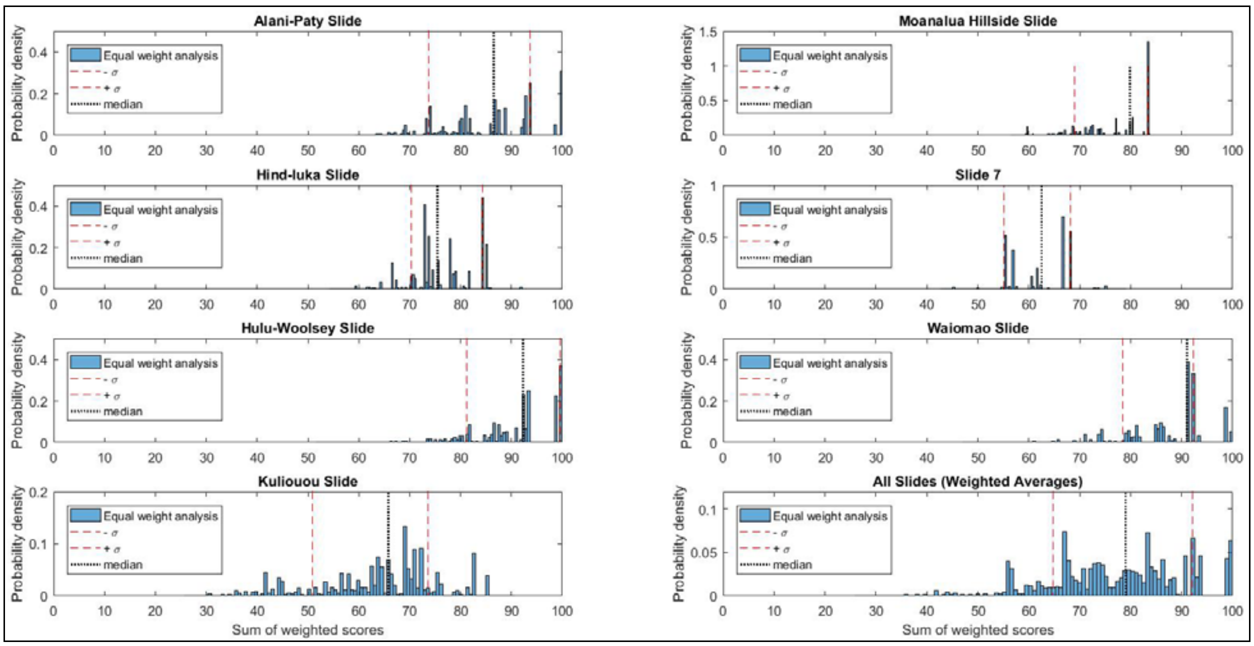

Figure 25. PDFs of the seven studied slide areas using the equal-weights susceptibility map. Dashed lines indicate the 15.9 and 84.1 percentiles corresponding to ± a standard deviation σ for a normal distribution. Vertical scales vary.

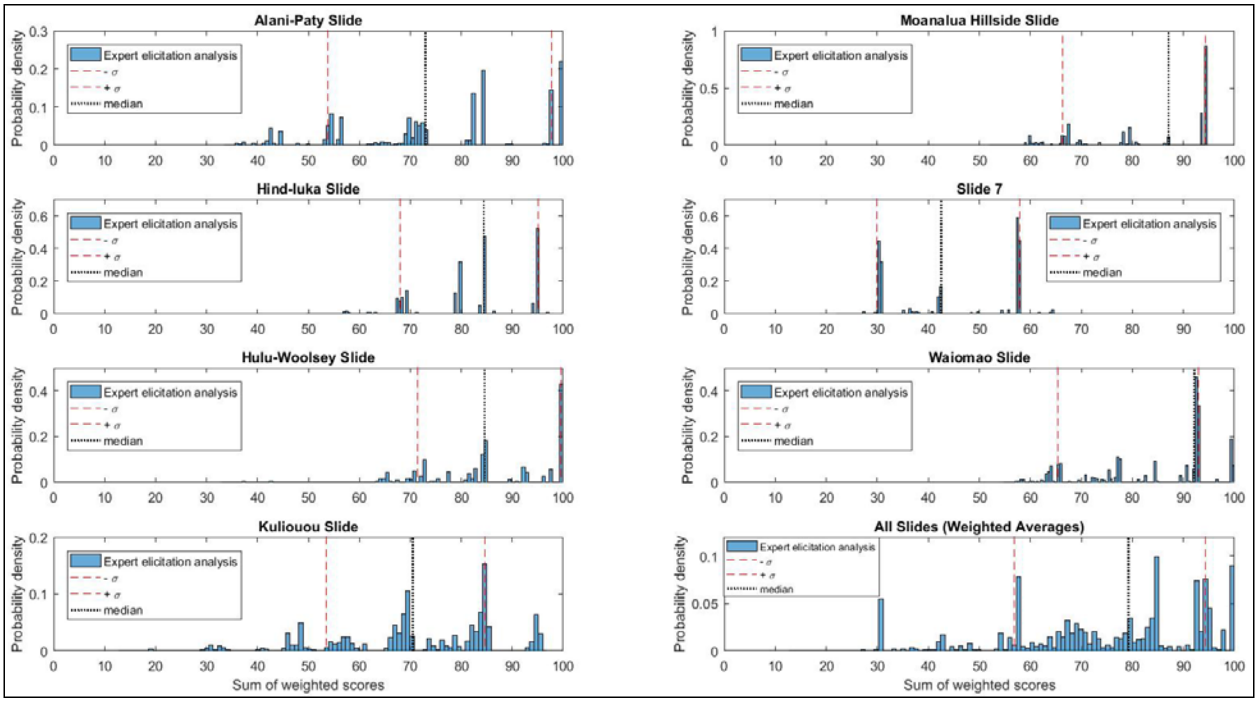

Figure 26. Same **as Figure 27, but for the expert elicitation susceptibility map. Vertical scales vary.**

Table 12. Median “Sums of weighted scores” for the seven studied slides, based on susceptibility maps.

Slide	**Median "Sum of weighted scores" from equal weight analysis**	**Median "Sum of weighted scores" from Expert elicitation analysis**
Alani-Paty	86.6	73.0
Hind-Iuka	75.5	73.0
Hulu-Woolsey	92.3	84.6
Kuliouou	65.8	70.5
Moanalua Hillside	79.8	87.1
Slide 7	62.5	42.5
Waiomao	91.0	92.2
All slides (average from random sampling)	**79.0**	**79.3**

We then revised the susceptibility maps according to these susceptibility categories. Figure 27 shows the categorized susceptibility map of the equally weighted parameters, and Figure 28 shows the categorized susceptibility map of the expert elicitation. The areas of high susceptibility are approximately the same in the two maps, whereas the expert elicitation map shows greater areas of medium susceptibility. The expert elicitation susceptibility map shows a greater area overall as either high or medium susceptibility (combined). This result is different from a comparison of Figure 23 to Figure 24, which appeared to show larger areas of intermediate values of raw susceptibility (yellow) in the equal weight analysis (and included valley floors as moderately susceptible in the equal weight analysis). The reason for the difference is that the categorization displayed in Figures 27-28 is based on the 15.9 percentile and the median, whereas in Figures 23-24, the colors are based on the raw sums of weighted scores.

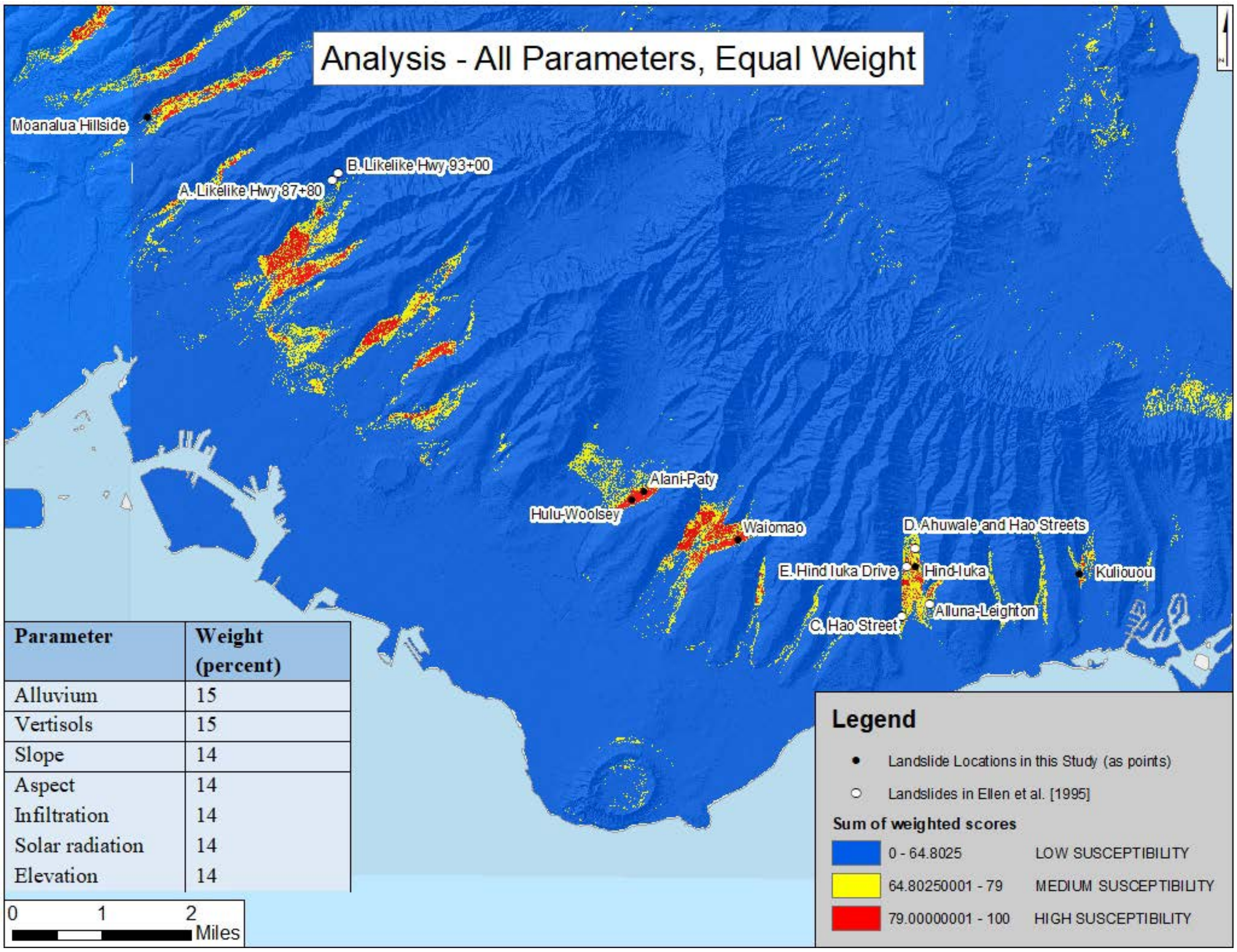

Figure 27. Susceptibility map of all seven parameters, weighted equally.
Blue represents low susceptibility, yellow represents medium, and red represents high.

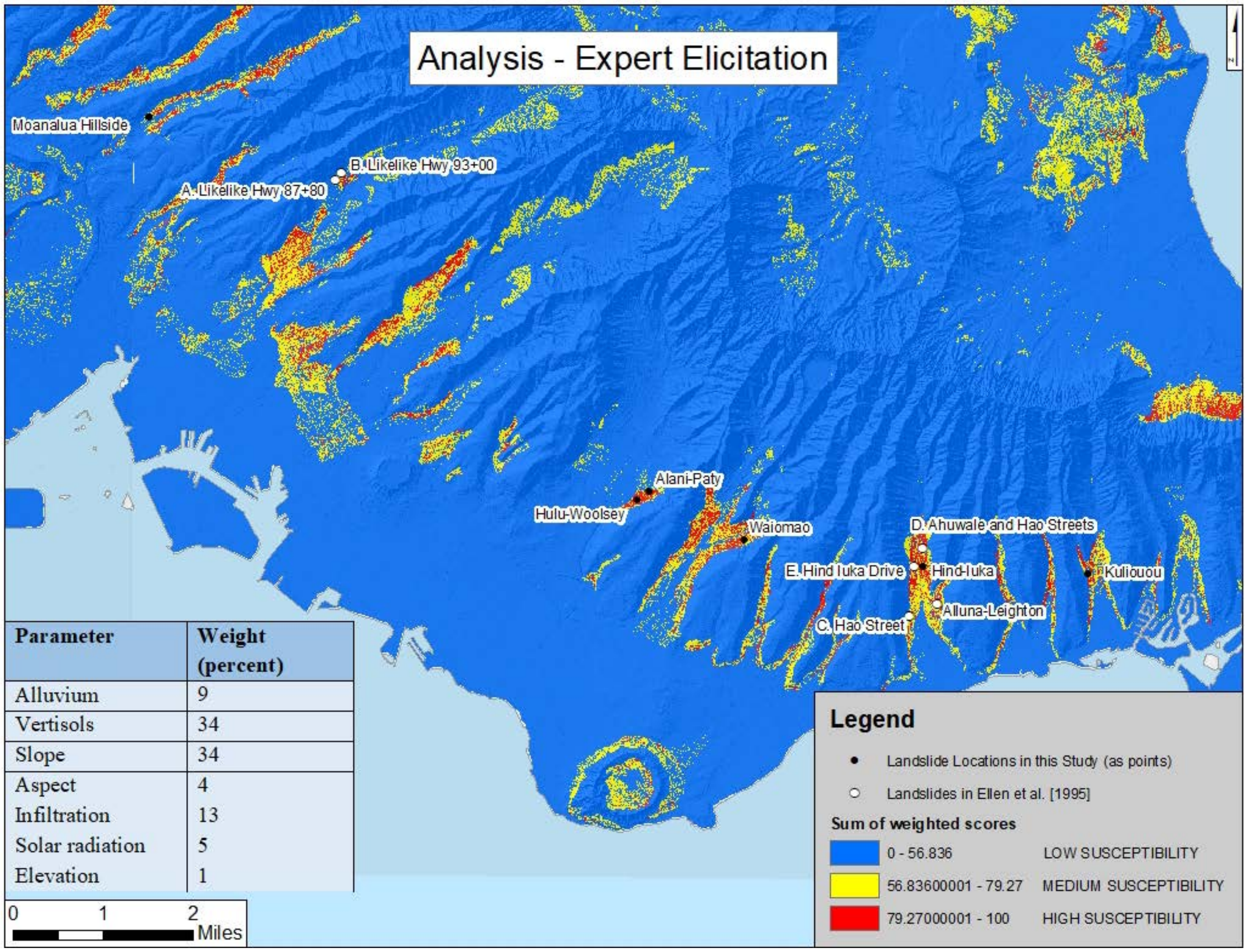

Figure 28. Susceptibility map based on expert elicitation.
Blue represents low susceptibility, yellow represents medium, and red represents high.

Figures 29 through 35 show the two categorized susceptibility maps side-by-side for each of the seven studied slides. A review of these comparisons provides a visual evaluation of the variation that may be expected at other areas with medium to high susceptibility. In some cases, the equal weight susceptibility maps appears to be a slightly better indicator of a slow-moving landslide (Alani-Paty, Hulu-Woolsey, and Waiomao). In other cases (Hind-Iuka and Kuliouou), the expert elicitation is a noticeably better predictor. For the other two slides (Moanalua Hillside and Slide 7), the two susceptibility maps are very similar.

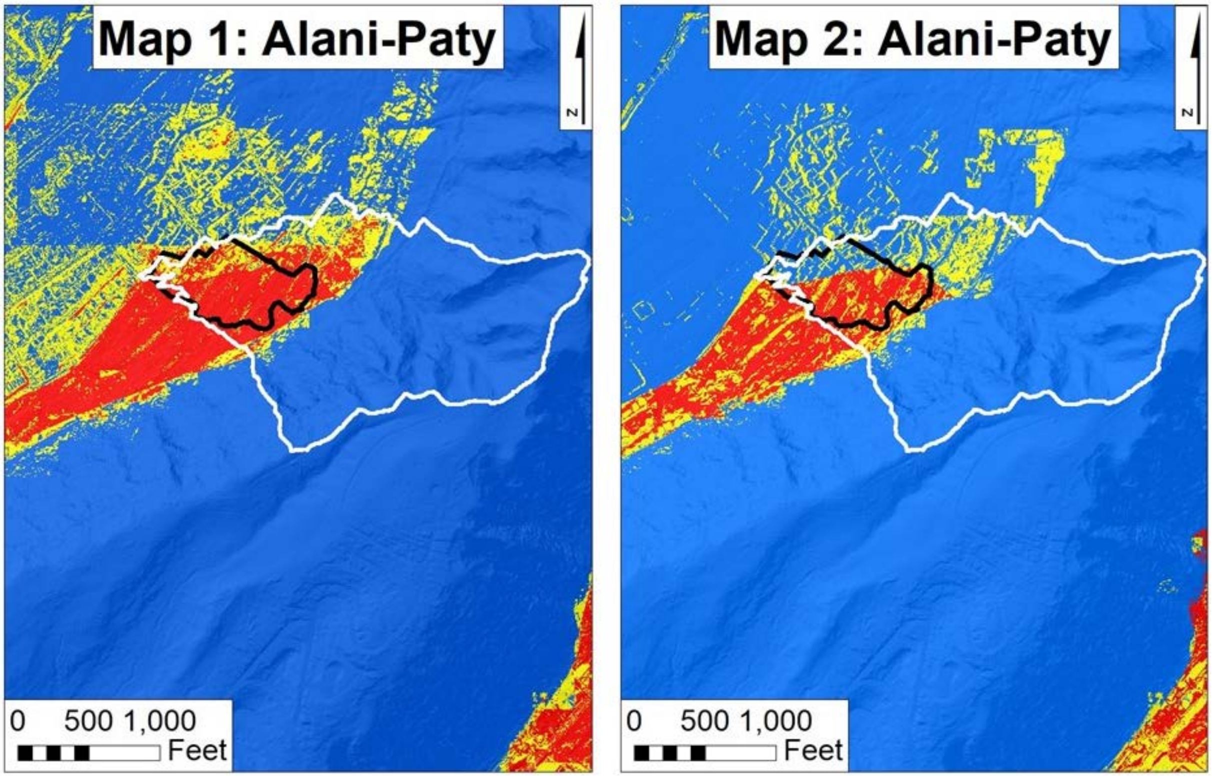

Figure 29. Alani-Paty slide with categorized susceptibility maps.
Map 1 is the equal weight susceptibility map and Map 2 is the expert elicitation.

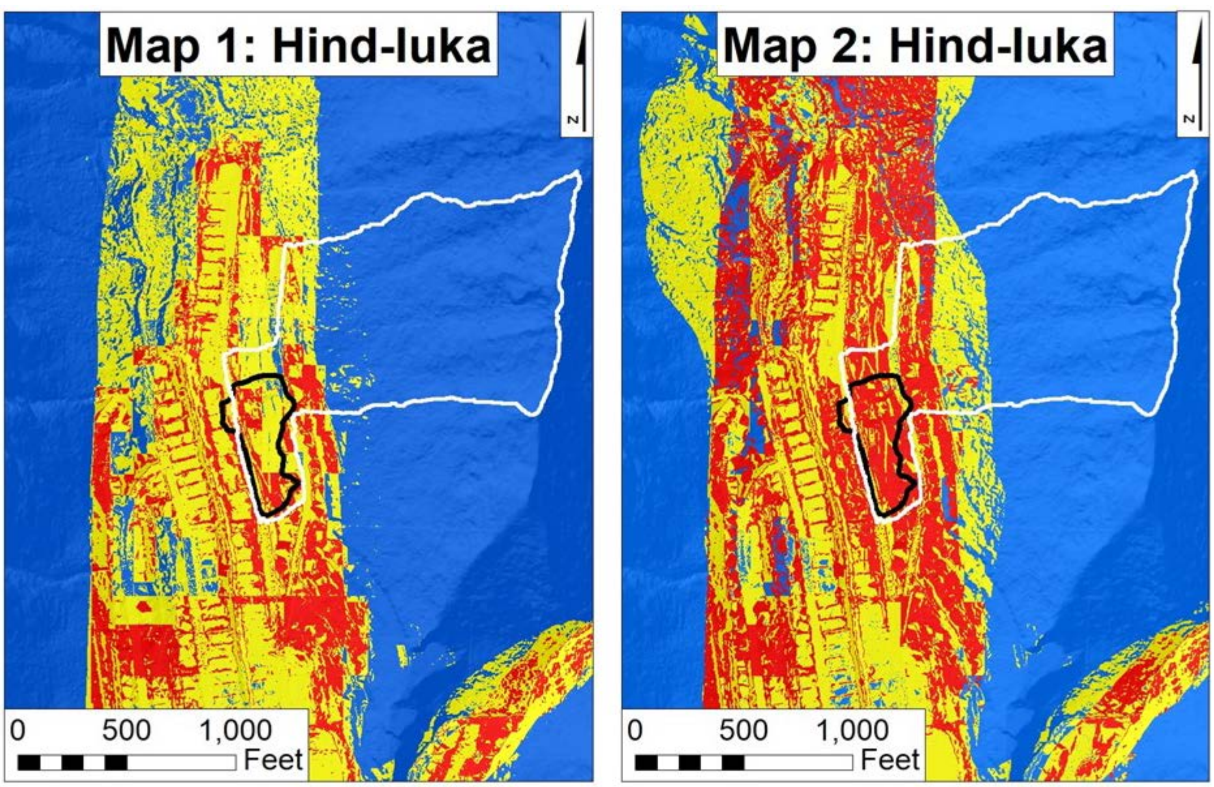

Figure 30. Hind-Iuka slide with categorized susceptibility maps.
Map 1 is the equal weight susceptibility map and Map 2 is the expert elicitation.

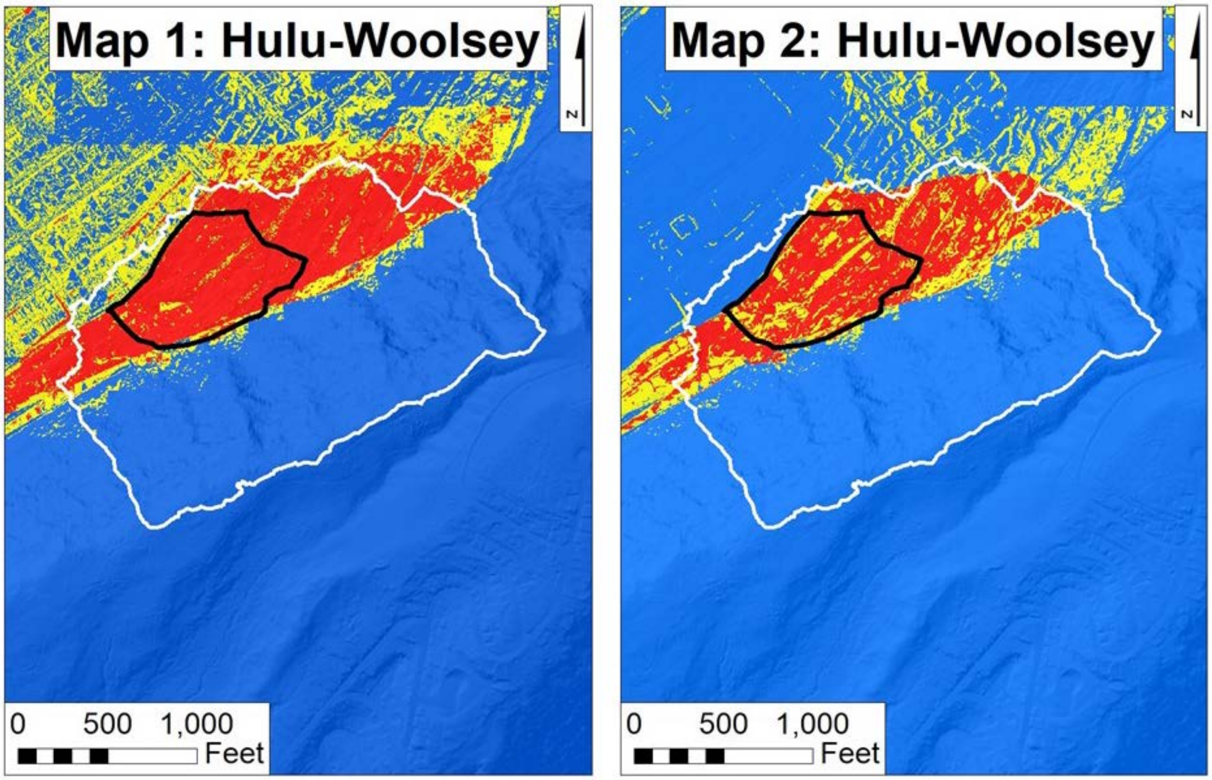

Figure 31. Hulu-Woolsey slide with categorized susceptibility maps.
Map 1 is the equal weight susceptibility map and Map 2 is the expert elicitation.

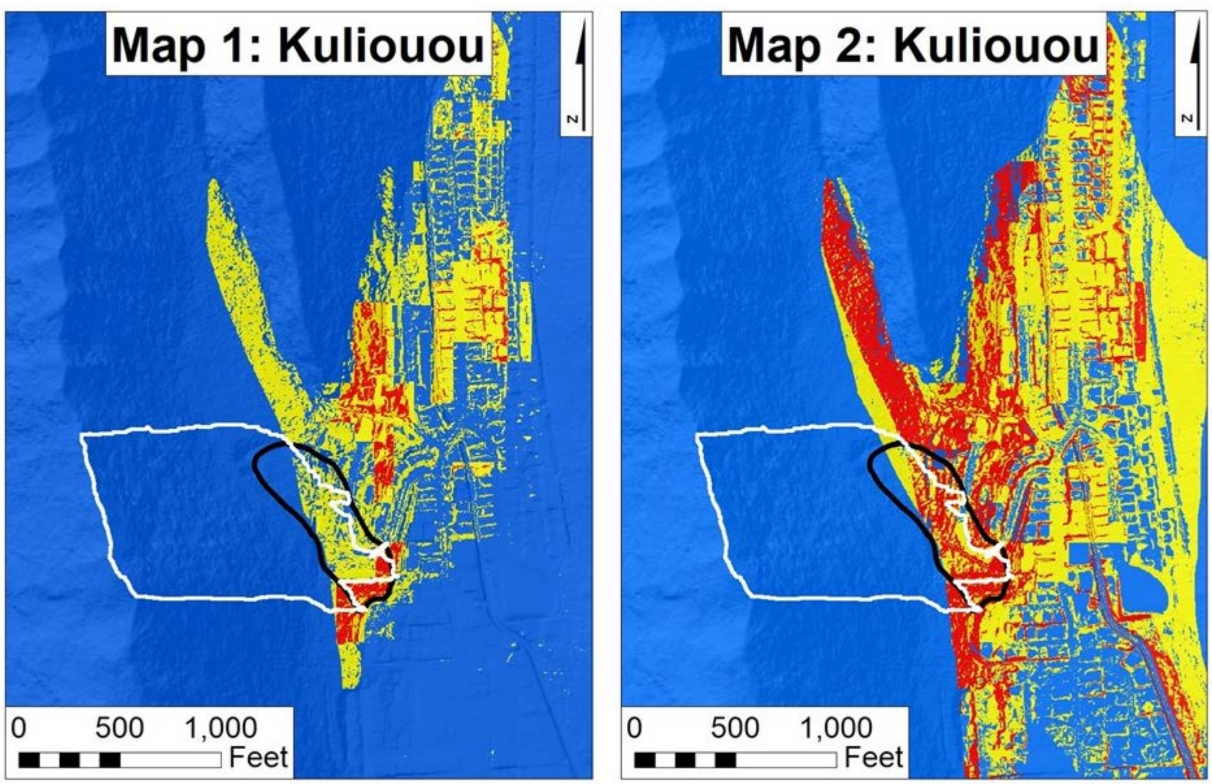

Figure 32. Kuliouou slide with categorized susceptibility maps.
Map 1 is the equal weight susceptibility map and Map 2 is the expert elicitation.

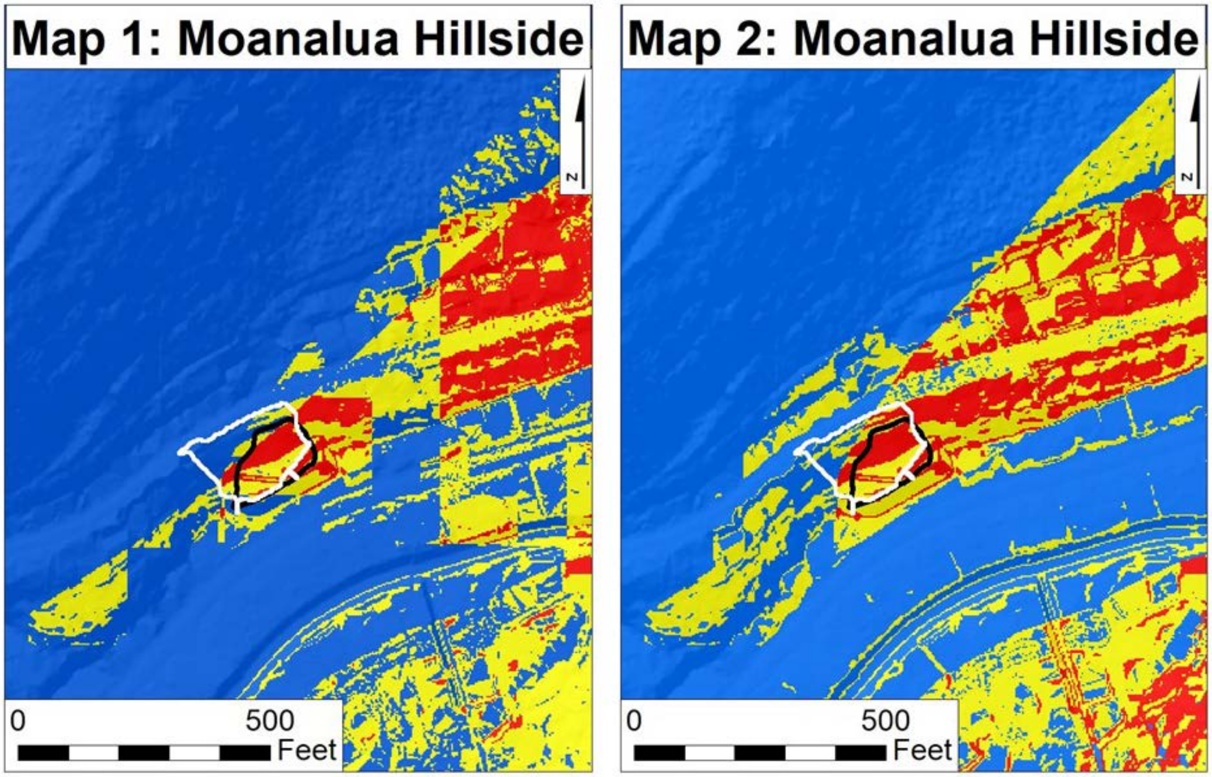

Figure 33. Moanalua Hillside slide with categorized susceptibility maps.
Map 1 is the equal weight susceptibility map and Map 2 is the expert elicitation.

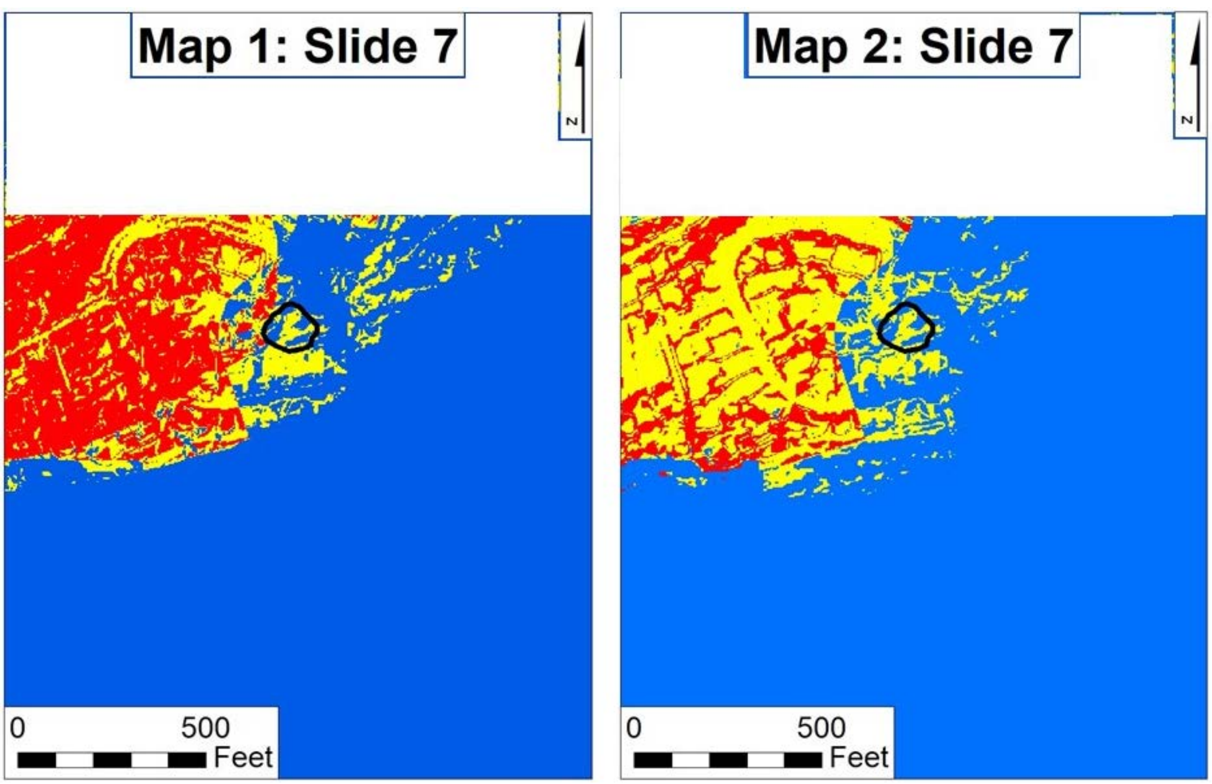

Figure 34. Slide 7 with categorized susceptibility maps.
Map 1 is the equal weight susceptibility map and Map 2 is the expert elicitation.

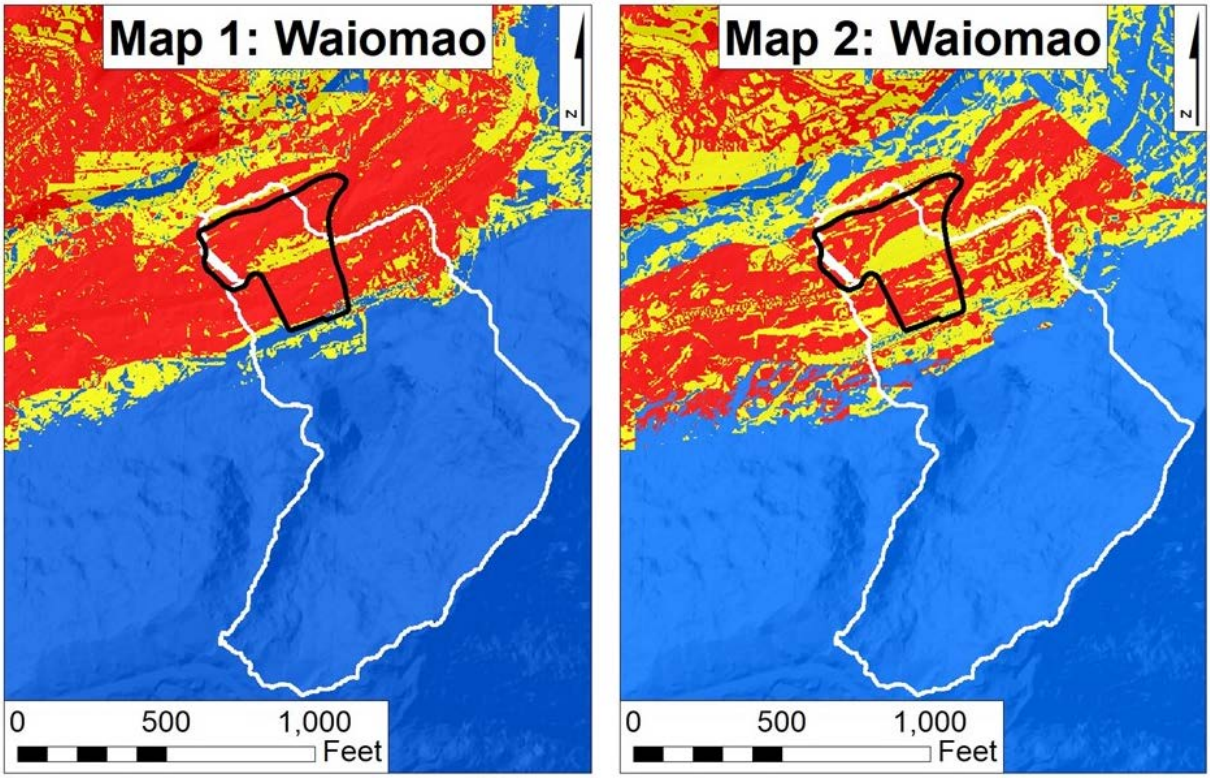

Figure 35. Waiomao slide with categorized susceptibility maps.
Map 1 is the equal weight susceptibility map and Map 2 is the expert elicitation.

5.0 EVALUATIONS OF SUSCEPTIBILITY MAPS AND CONCLUSIONS

To evaluate the performance of our categorized susceptibility maps, we examined the predictions within each of the seven slides of this study as well as the other slides considered by *Ellen et al.* [1995]. Of the six slides in *Ellen et al*. [1995] that were not part of our study, two are currently known: Ailuna-Leighton; and “C”, Hao Street, which is near the intersection of Aipuni and Hao Streets [*De Silva*, 1974]. Therefore, these slides are excellent candidates for evaluating our susceptibility maps. The other four slides – “A”, “B”, “D”, and “E” – may be used for the same purpose, but only with caution because it is not currently known if they are indeed slow-moving landslides.

Five of the slides identified in *Ellen et al.* [1995], “A” through “E”, could not be confirmed by the study authors because the land had been modified, but they were included in the study based on written descriptions in historical literature: UH PhD theses by *De Silva* [1974] and *Jellinger* [1977]. As indicated above, one of those five slides is now well known; however, it is not clear why the other four were singled out among the many dozens identified by De Silva and Jellinger, particularly “A”, Likelike Highway 87+80, and “D”, Ahuwale and Hao Streets, which were each reported by *De Silva* [1974] as a single slide event.

In order to use landslides identified in *Ellen et al.* [1995] to evaluate our susceptibility maps, we needed to confirm their locations. As part of our study, we had mapped six of the confirmed slides in *Ellen et al*. [1995]. The seventh of their confirmed slides, Ailuna-Leighton, is now well known. There are detailed location maps by *De Silva* [1974] of the other ‘Āina Haina slides in *Ellen et al.* [1995] (designated by them as “C”, “D”, and “E”). Once we had mapped the aforementioned slide locations, we used them to georeference Plate 1 from *Ellen et al*. [1995]. We then used the georeferenced Plate 1 to plot the locations of the remaining two slides, “A” and “B” (i.e. the Likelike Highway slides). The georeferencing has some inherent errors, particularly due to the scale of Plate 1, and the concentration of tie-points in only a few areas. Therefore, the locations of the Likelike Highway landslides are approximate.

We conducted a visual evaluation of our categorized susceptibility maps of the seven slides in our study (Figures 29-35) as well as for the six landslides in *Ellen et al*. [1995] that were not part of our study, based on the immediate vicinity of each plotted location. The results are summarized in Table 13.

Table 13. Slow-moving landslides mapped in our study and *Ellen et al.* [1995].

Slide name in this study	**Slide name in *Ellen et al*. [1995]**	**Source of information for historical slides mapped in *Ellen at al.* [1995]**	**Support for use to check predictive mapping**	**Susceptibility based on Equal Weights**	**Susceptibility based on Expert Elicitation**
Alani-Paty	Alani-Paty	--	Extensively studied slow-moving slide.	High	High
Hind Iuka	Hind Iuka	--	Extensively studied slow-moving slide.	Medium to high	High
Hulu-Woolsey	Hulu-Woolsey	--	Extensively studied slow-moving slide.	High	High
Kuliouou	Kuliouou	--	Extensively studied slow-moving slide.	Low to medium	Medium to high

Slide name in this study	Slide name in *Ellen et al*. [1995]	Source of information for historical slides mapped in *Ellen at al.* [1995]	Support for use to check predictive mapping	Susceptibility based on Equal Weights	Susceptibility based on Expert Elicitation
Moanalua Hillside	Moanalua Hillside	--	Extensively studied slow-moving slide.	Medium to high	Medium to high
Slide 7	--	--	Known by author; sliding has taken place over several years.	Low to medium	Low to medium
Waiomao	Waiomao	--	Extensively studied slow-moving slide.	High	High
--	Ailuna-Leighton	--	Well known slide area; several homes have been demolished.	Low to medium	Medium
--	A. Likelike Highway 87+80	*De Silva* [1974] slide #41 (pp.188-196)	None found; reported by De Silva as a single event.	Low	Low to medium
--	B. Likelike Highway 93+00	*De Silva* [1974] slide #42 (pp.188-196)	None found, but description by De Silva suggests a slow-moving slide.	Low	Low to medium
--	C. Hao Street	*De Silva* [1974] slide #7 (pp.232-236); *Jellinger* [1977] p.116	Some lots are empty, suggesting that houses have been demolished.	Medium	Medium to high
--	D. Ahuwale	*De Silva* [1974] slides #4 & 5 (pp.	None found; reported by De	Medium	High

Slide name in this study	**Slide name in *Ellen et al*. [1995]**	**Source of information for historical slides mapped in *Ellen at al.* [1995]**	**Support for use to check predictive mapping**	**Susceptibility based on Equal Weights**	**Susceptibility based on Expert Elicitation**
	and Hao Streets	237-238); *Jellinger* [1977] p.116	Silva as a single event.		
--	E. Hind Iuka Drive	*De Silva* [1974] slide #3 (pp. 237-238); *Jellinger* [1977] p.116	Lots are currently empty, suggesting that houses have been demolished.	Medium	Medium to high

In general, the susceptibility map produced from expert elicitation does a better job of predicting slow-moving landslides compared to the susceptibility map produced using equal weights. If we ignore the two Likelike Highway slides – which may not be slow-moving slides – then the expert elicitation susceptibility map generally performs well, based on the comparison to the other known landslides that area in *Ellen at al.* [1995] but not included in our study. Slide 7 appears to be the one other outlier, which is not well predicted. In general, the equal weight susceptibility map performs poorly to moderately well.

The comparison of our susceptibility maps to known slow-moving landslides suggests that the maps produced in our study are not precise enough for use on the scale of individual lots or even neighborhoods. The maps are better for assessing the susceptibility of broader areas and therefore the degree that owners, engineers, and developers should investigate individual sites in more detail.

As a final step, we developed an island-scale map, with the weighting of the Expert Elicitation (Figure 36). This map is more general than the susceptibility maps previously displayed, because the island-wide slope, aspect, and elevation rasters were produced from a 10-meter DEM. However, large red areas suggest that certain regions on the island – many of which are currently undeveloped – may be highly susceptible to slow-moving landslides.

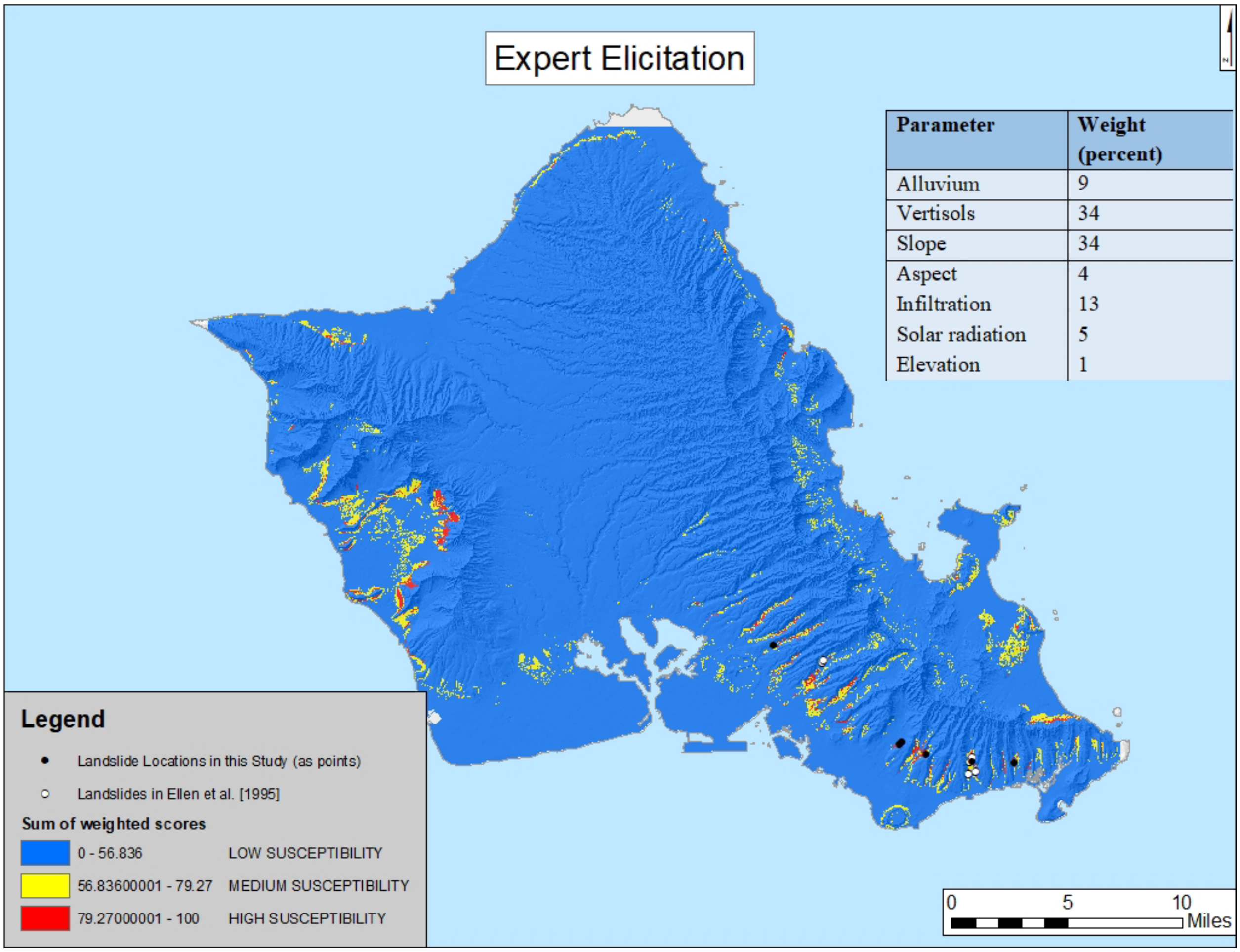

Parameter	Weight (percent)
Alluvium	9
Vertisols	34
Slope	34
Aspect	4
Infiltration	13
Solar radiation	5
Elevation	1

Figure 36. Island-wide Slow-Moving Landslide Susceptibility Map with weights provided through Expert Elicitation.
A 10-m DEM was used.

6.0 LIMITATIONS AND RECOMMENDATIONS FOR ADDITIONAL STUDY

Our susceptibility maps should be used with caution, particularly on a localized scale, due to the subjective nature of weighting the parameters as well as the variable resolution and margins of error associated with the different data types (Table 3). Additionally, the DEM-derived layers used in the island-wide mapping are based on 10-meter DEMs, and therefore have lower resolution.

A major limitation in the use of these analyses on the scale of individual lots and even neighborhoods is the weighting of the parameters. An interesting follow-up study could focus on a single neighborhood where there is a known slow-moving landslide that was not part of our study. A variety of weights can be tried for the one neighborhood to constrain the weights based on the known slide area.

At the outset of our study, attempts were made to obtain subsurface data: all the prominent geotechnical engineering firms on island were contacted, along with the City & County of Honolulu (CCH) Department of Design and Construction (DDC), and the USGS. Whereas engineering firms would have been willing to assist, they were unable to provide data because of the proprietary nature. DDC declined to provide data or reports that were not in the files of the Municipal Reference Center (MRC), which has a repository of approved geotechnical reports prepared by consultants under contract with the CCH. DDC indicated that draft reports are not available to the public until they are approved. Reports filed in the MRC were limited, and it appeared that inclusion of reports in the MRC is haphazard: it was not uncommon to find a progress report Number 12 or even Number 21 with no preceding reports. Reports are typically sent to individuals within the DDC, leaving it to the individual to provide them to the MRC; however, there does not appear to be a requirement to do so. Further, the MDC has recently disposed of many of the geotechnical reports they had on file in print copy; these were collected by the UH’s Hawai‘i Institute of Geophysics & Planetology (HIGP) and are being scanned. USGS has not prepared any reports on slow-moving landslides in Hawai‘i since the mid-1990s; the reports from then were available and some contained limited subsurface data. The State of Hawai‘i is one of the few states that lack a State Geological Survey, and there is no single repository of geologic or geotechnical data on the island. Such a repository would make future studies of slow-moving landslides (and any geologic hazards, for that matter) much easier to conduct. The creation of an agency with oversight of geologic hazards in the State, and to whom other agencies are required to provide their geologic and geotechnical reports, would be of primary importance in promoting public safety from geologic hazards.

Finally, the presence of a high percentage of amorphous silica-rich material in the clay-sized fraction of soils may be a driving factor in the development of slow-moving landslides. It is unknown if mapping of surficial parameters can reflect their likely presence. This topic could provide an interesting future study. Such a study would require sample collection and x-ray diffraction analysis at multiple sites.

7.0 ACKNOWLEDGEMENTS

This project could not have been completed without the assistance of many people. We would particularly like to thank the following individuals, who have been instrumental in the completion of the project: Advisor Dr. Garrett Apuzen-Ito (UH Geology & Geophysics faculty member) for his invaluable guidance, wisdom, encouragement, and infinite patience; committee member, Dr. Scott Rowland (UH Geology & Geophysics faculty member) for his time, insights and GIS assistance; committee member, Mr. Masa Fujioka (Managing Principal, Masa Fujioka & Associates) for agreeing to a reduced work schedule and very flexible hours that accommodated course attendance and time to work on this study; and Mr. Craig Clouet at the Esri Honolulu office for providing GIS data, suggestions on which ArcGIS tools to use and instruction on how to use them, and responding to innumerable GIS questions. Geotechnical engineers and geologists at several local firms and UH College of Engineering contributed time to discuss project ideas and the availability of data, and in some cases provided studies they have conducted. Ms. Robin Ballentyne at the City and County of Honolulu Municipal Reference Center scanned several reports that had previously been available in hard copy only and unavailable for loan outside of the MRC building. Staff at USGS Honolulu assisted with interpretation of climate data. Dr. Rex Baum of the USGS, who had formerly been with the Honolulu district and involved with the slow-moving landslide research in the 1980s and 1990s, suggested the idea for the project.

8.0 REFERENCES

Baum, R.L., and Reid, M.E. 1992. Geology, hydrology, and mechanics of the Alani-Paty landslide, Manoa Valley, Oahu, Hawaii. U.S. Geological Survey Open-File Report 92-501, 87 p. 6 plates. Online at https://pubs.er.usgs.gov/publication/ofr92501.

Baum, R.L., and Reid, M.E. 1995. Geology, hydrology, and mechanics of a slow-Moving, Clay-Rich Landslide, Honolulu, Hawaii, in Haneberg, W.C., and Anderson, S.A., eds., Clay and Shale Slope Instability: Boulder, Colorado, Geological Society of America Reviews in Engineering Geology, v. X.

Brandes, H.G. 2012. Slope Hazards Investigation, 510 Kuli‘ou‘ou Road, TMK: 3-8-010:004, Project No. SRSS00110. Obtained from Author.

College of Tropical Agriculture and Human Resources, University of Hawai‘i. 2014. Hawaii Soil Atlas. [Derived from the Natural Resources and Conservation Service (NRCS) databases and websites]. Online at http://gis.ctahr.hawaii.edu/SoilAtlas#acks.

Deb, S.K., and El-Kadi, A.I. 2009. Susceptibility assessment of shallow landslides on Oahu, Hawaii, under extreme-rainfall events. J. of Geomorphology, 108: 219–233. Online Copy: doi: 10.1016/j.geomorph.2009.01.009.

De Silva, GLR. 1974. Slope stability problems induced by human modification of the soil covered hill slopes of Oahu, Hawaii. UH PhD dissertation, Geography.

Ellen, S.D., Liu, L.A.S.M., Fleming, R.W., Reid, M.E., and Johnsson, M.J., Relation of slow-moving landslides to earth materials and other factors in valleys of the Honolulu District of Oahu, Hawaii: U.S. Geological Survey Open-File Report 95-218, 45 p., 2 maps (1:40,000). Online at https://pubs.er.usgs.gov/publication/ofr95218.

Engott, John A. 2017. Mean annual water-budget components for the Island of Oahu, Hawaii, for average climate conditions, 1978-2007 rainfall and 2010 land cover (version 2.0) [GIS shapefile]. U.S. Geological Survey Scientific Investigations Report 2015-5010. https://water.usgs.gov/lookup/getspatial?sir2015-5010_Oahu_WB_components_avg_climate.

Engott, J.A., Johnson, A.G., Bassiouni, Maoya, Izuka, S.K., and Rotzoll, Kolja. 2017. Spatially distributed groundwater recharge for 2010 land cover estimated using a water-budget model for the Island of O‘ahu, Hawai‘i (ver. 2.0, December 2017): U.S. Geological Survey Scientific Investigations Report 2015–5010, 49 p., https://doi.org/10.3133/sir20155010.

Geolabs. 2015. Monitoring Progress Report No. 28, Phase III - Additional Instrumentation Monitoring, Kuahea Street Area Movement; CIP Project No. 97504, Contract No. 60578, Amendment No. 14; Palolo, Oahu, Hawaii. Prepared for City & County of Honolulu Department of Design & Construction. Obtained from the City & County of Honolulu Municipal Reference Center.

Giambelluca, T.W., Q. Chen, A.G. Frazier, J.P. Price, Y.-L. Chen, P.-S. Chu, J.K. Eischeid, and D.M. Delparte. 2013. Online Rainfall Atlas of Hawai‘i. Bull. Amer. Meteor. Soc. 94, 313-316, doi: 10.1175/BAMS-D-11-00228.1. http://rainfall.geography.hawaii.edu/downloads.html

Giambelluca, T.W., X. Shuai, M.L. Barnes, R.J. Alliss, R.J. Longman, T. Miura, Q. Chen, A.G. Frazier, R.G. Mudd, L. Cuo, and A.D. Businger. 2014. Evapotranspiration of Hawai‘i. Final report submitted to the U.S. Army Corps of Engineers—Honolulu District, and the Commission on Water Resource Management, State of Hawai‘i. http://solar.geography.hawaii.edu/.

Jellinger, Moanikeala. 1977. Methods of detection and analysis of slope instability, southeast Oahu, Hawaii. UH PhD dissertation, Agronomy and Soil Science.

Kaya, A., and Kwong, J.K.P., 2007. Evaluation of common practice empirical procedures for residual friction angle of soils: Hawaiian amorphous material rich colluvial soil case study. Engineering Geology 92, 49–58.

Lyon Associates, Inc. 2014, January 3. Geotechnical Instrument Monitoring, Woodlawn Area Earth Stabilization, October 2011 - September 2012. Prepared for Department of Design and Construction, City and County of Honolulu. Obtained from the City & County of Honolulu Municipal Reference Center.

Lyon Associates, Inc. 2015, December 18. Final. Geotechnical Instrument Monitoring, Moanalua Valley Hillside Repairs, October 2013 through September 2014; Amendment No. 26 to Contract No. F-57540. Prepared for Department of Design and Construction, City and County of Honolulu. Obtained from the City & County of Honolulu Municipal Reference Center.

National Geospatial-Intelligence Agency. 2009a. Lidar-derived bare earth Digital Elevation Model (DEM) titled “honolulu_be_southeast”. Provided by Esri Honolulu. No metadata available.

National Geospatial-Intelligence Agency (NGA). 2009b. Lidar-derived bare earth Digital Elevation Model (DEM) titled “honolulu_be_southwest”. Provided by Esri Honolulu. No metadata available.

O’Hagan, A., Buck, C.E., Daneshkhah, A., Eiser, J.R., Garthwaite, P.H., Jenkinson, D.J., Oakley, J.E., Rakow, T., 2006. Uncertain Judgements: Eliciting Expert Probabilities. Wiley, United Kingdom.

O’Leary, R.A., Choy, S.L., Murray, J.V., Kynn, M., Denham, R., Martin, T.G., Mengersen, K., 2009. Comparison of three expert elicitation methods for logistic regression on predicting the presence of the threatened brush-tailed rock-wallaby Petrogale penicillata. Environmetrics 20, 379–398.

Peck, R. 1959, December. Report on Causes and Remedial Measures, Waiomao Slide, Honolulu. 33p.

Peck, R., 1968. The Hind Iuka Landslide and Similar Movements, Honolulu, Hawaii, 22p.

Sherrod, D.R., Sinton, J.M., Watkins, S.E., and Brunt, K.M. 2007. Geologic Map of the State of Hawaiʻi. Open-File Report 2007-1089. United States Geological Survey. Online at https://pubs.usgs.gov/of/2007/1089/.

United States Department of Agriculture Soil Conservation Service [in cooperation with The University of Hawaii Agricultural Experiment Station]. 1972. Soil Survey of Islands of Kauai, Oahu, Maui, Molokai, and Lanai, State of Hawaii. Washington, DC: U.S. Government Printing Office.

United States Department of Agriculture, Natural Resources Conservation Service. September 27, 2012 (Version 7). Soil Survey Geographic (SSURGO) database for Island of Oahu [area hi990]. Retrieved July 11, 2013 from http://websoilsurvey.nrcs.usda.gov/.

United States Geological Survey 2015. USGS 10-m Digital Elevation Model (DEM): Hawaii: Oahu Provided by Esri Honolulu.

Wan, Yongshan, and Kwong, James. 2002. Shear Strength of Soils Containing Amorphous Clay-Size Materials in a Slow-Moving Landslide. Engineering Geology 65 (002) 293-303.

Wan, Yongshan, Kwong, James, Brandes, Horst G., and Jones, Rollin C. 2002, December. Influence of Soils Amorphous Clay-Size Materials on Soil Plasticity and Shrink-Swell Behavior. Journal of Geotechnical and Geoenvironmental Engineering 1026-1031.